PAPER

Check for updates

Sorption and biodegradation of stormwater trace organic contaminants *via* composite alginate bead geomedia with encapsulated microorganisms†

Debojit S. Tanmoy[ab] and Gregory H. LeFevre (iD) *[ab]

Urban areas generate high volumes of stormwater runoff that frequently contains complex mixtures of hydrophilic trace organic contaminants (TOrCs) and dissolved nutrients. Green stormwater infrastructure is becoming increasingly adopted as a nature-based solution for improving water quality but is typically inefficient for removing dissolved-phase contaminants. We recently developed and characterized novel bioactive composite alginate bead media (BioSorp Beads) containing encapsulated PAC and iron-based water treatment residuals [FeWTR] as sorbents and white rot fungi as model biodegrading organisms to effectively capture and biodegrade stormwater-relevant TOrCs. We created multiple abiotic (no fungi) and biotic beads (containing *Trametes versicolor* or *Pleurotus ostreatus* fungi) to investigate sorption removal of a suite of representative dissolved-phase stormwater relevant pollutants (a neonicotinoid/metabolite, phosphate, three PFAS, and one tire-wear compound [acetanilide]). We also measured coupled sorption and biodegradation of acetanilide as a proof-of-concept demonstration of encapsulated biodegrading organisms. Alginate encapsulation increased desnitro-imidacloprid sorption onto PAC, likely due to the interactions between compound altered insecticidal functional groups and alginate. The sorption capacity of imidacloprid and desnitro-imidacloprid was up to 29.1 mg g^{-1} and 16.8 mg g^{-1}, respectively, and impacted by PAC presence and the partial charge distributions of the compounds. The encapsulated FeWTR and Fe^{3+}-alginate beads drove phosphate sorption (42.1 mg phosphate per g beads). Long-chain PFAS removal in the beads (13.1 mg PFOA per g) was greater than short-chain PFAS removal capacity (5.2 mg PFBA per g, 5.1 mg PFBS per g). Encapsulated fungi were not inhibited by exposure to azide that typically kill fungi in laboratory experiments, indicating the potential for encapsulation to protect organisms from harsh conditions. Furthermore, biodegradation of acetanilide by encapsulated fungi beyond sorption controls demonstrated that coupled sorption and biodegradation with the beads occurred. BioSorp Beads successfully capture and biodegrade representative hydrophilic stormwater TOrCs and thus hold potential as a green stormwater infrastructure geomedium and bioaugmentation tool.

Water impact

Incorporating biologically active sorption geomedia into green stormwater infrastructure could effectively capture and sustainably degrade hydrophilic trace organic contaminants and dissolved nutrients from urban stormwater runoff. The geomedia successfully sorbed a suite of stormwater-relevant contaminants, including urban-use insecticides, tire-wear compounds, PFAS, and dissolved nutrients. We also demonstrate coupled sorption and biodegradation of a tire-wear compound (acetanilide) *via* encapsulated fungi.

1. Introduction

[a] Department of Civil and Environmental Engineering, University of Iowa, 4105 Seamans Center, Iowa, 52242, USA. E-mail: gregory-lefevre@uiowa.edu; Tel: +319 335 5655

[b] IIHR—Hydroscience and Engineering, University of Iowa, 100 C. Maxwell Stanley Hydraulics Laboratory, Iowa, 52242, USA

† Electronic supplementary information (ESI) available. See DOI: https://doi.org/10.1039/d4ew00600c

Urban areas generate rapid and intense stormwater runoff during rain events and/or after snow-melts due to the substantial proportions covered with impervious surfaces.[1–3] Stormwater runoff frequently contains complex mixtures of nutrients, metals, microplastics, and trace organic contaminants (TOrCs) that impact surface water and groundwater.[3,4] Moderate to high concentrations of TOrCs

This journal is © The Royal Society of Chemistry 2024

Environ. Sci.: Water Res. Technol., 2024, **10**, 3339–3357 | **3339**

including pesticides (*e.g.*, urban use herbicides and insecticides used in landscaping), biocides (*e.g.*, leached from building materials), hydrocarbons (*e.g.*, from vehicular oil leaks, road construction materials), vehicular fluids and solvents, and tire and road wear compounds are commonly found in urban stormwater runoff.[5–9] These complex mixtures of contaminants can pose risks to human and ecological health.[4,10–12] For instance, tire-wear compounds such as acetanilide, 1,3-diphenylguanidine [DPG], and *N*-(1,3-dimethylbutyl)-*N'*-phenyl-*p*-phenylenediamine [6PPD] are common in urban stormwater runoff and can harm the environment.[13] One of the transformation products of 6PPD causes acute coho salmon mortality (transformation product: 2-anilino-5-[(4-methylpentan-2-yl)amino]cyclohexa-2,5-diene-1,4-dione [6PPD-quinone]).[14] Dissolved nutrients (*e.g.*, N-containing compounds, phosphate) can also lead to eutrophication of receiving waters and hydrophilic pesticides can exert toxicity towards nontarget organisms.[15–20] Stormwater runoff from airports, industries, military bases, firefighting sites, and landfills are known to contain multiple types of harmful PFAS 'forever chemicals',[21,22] which can eventually impact drinking water sources.

Green stormwater infrastructure (GSI) is a nature-based solution designed to improve urban runoff quality, manage flooding, and replenish groundwater.[23,24] GSI implementation is becoming increasingly popular because GSI is cost-effective and can remove a wide variety of non-point source pollutants—transforming stormwater from a waste into a valuable resource.[25] GSI can also help address some social/environmental justice issues in communities, enhance city aesthetics, increase property values, provide microhabitats for different pollinators, and improve water quality for human and urban wildlife.[25,26] GSI such as bioretention cells are designed to accommodate rapid infiltration during storm events (to avoid extended ponding) and media generally consist of high-hydraulic conductivity gravel, soil, sand, compost, and mulch with vegetation.[23] Most bioretention cells are highly effective at capturing particle-bound contaminants (*e.g.*, suspended solids, pathogens, several nutrients [*e.g.*, particulate P], metals, *etc.*), but these practices are inadequate for many hydrophilic TOrCs and dissolved phase nutrients.[4,12,27,28] Composts are often used in conventional bioretention cells to increase bioretention infiltration rates, support plant growth, and sorb hydrocarbons and heavy metals.[29] Nevertheless, composts within the bioretention cell can leach and export dissolved nitrogen and phosphorus.[29] Amending bioretention media with sorptive materials such as black carbons,[30–33] iron enhanced sand,[34] or water treatment residuals[30,35–37] can increase sorption removal of these dissolved contaminants. Indeed, Rodgers *et al.*[38] demonstrated that bioretention design modification *via* sorptive material amendment (*e.g.*, adding black carbon into the system) can improve effluent water quality. Analogously, Zhang *et al.*[29] recommended using water treatment residuals (WTRs) in bioretention cells to increase dissolved phosphorus nutrient removal. Unlike

compost, sorptive geomaterials (*e.g.*, black carbon, WTR) generally reduce nutrient leaching in soil.[39] Nevertheless, even introduction of sorptive materials in bioretention cells cannot fully sustain stormwater contaminant removal because sorption capacity can eventually be exhausted and contaminants potentially break through to contaminate groundwater.[4,27,40,41]

Hence, combining contaminant capture with *in situ* biodegradation of stormwater contaminants is becoming increasingly appreciated as an approach to renew and sustain pollutant removal. One key challenge to achieving TOrC biodegradation in bioretention cells is associated with reconciling the short hydraulic residence time (HRT) of the system with the longer chemical residence time (CRT) required for contaminant biodegradation. Bioactive sorptive geomedia could potentially decouple the HRT and the CRT in stormwater—analogous to how activated sludge transformed wastewater treatment by separating HRT and solid residence time (SRT) as process parameters. Specifically, we posit that bioactive sorptive geomedia could promote effective chemical removal during rapid stormwater infiltration with subsequent biodegradation of captured TOrCs during the longer antecedent inter-event periods to sustain contaminant removal *in situ*. Bioaugmentation of GSI using geomedia containing beneficial microorganisms could biodegrade captured TOrCs *via* the sorptive materials present in the media during inter-storm periods, thereby extending GSI service life by renewing the sorption capacities of the geomedia.[42] Some types of fungi (*e.g.*, white rot) are capable of biodegrading recalcitrant organic contaminants due to their strong inter- and extracellular enzymes; for example, we previously demonstrated that *Trametes versicolor* is capable of biodegrading some tire-wear compounds and urban-use pesticides relevant to stormwater.[13,43] Although some types of fungi are present in stormwater bioretention cells,[44] there is potential to improve *in situ* biodegradation of recalcitrant trace organic contaminants through bioaugmentation of beneficial fungi to renew geomedia.

We recently developed a novel bioactive geomedium (a multi-material composite alginate bead, dubbed BioSorp Beads) that can be used in GSI systems to deploy contaminant-degrading microorganisms (*i.e.*, bioaugmentation) and sustain contaminant removal *via* sorption and potential biodegradation.[45] Briefly, we encapsulated two types of sorbents (powdered activated carbon [PAC] and iron water treatment residual [FeWTR; also increases bead density]), a representative biodegrading organism (white rot fungi [WRF]; *T. versicolor* or *Pleurotus ostreatus*), a maintenance substrate (wood flour [WF]), and a model electron shuttling compound (anthraquinone-2,6-disulfonate [AQDS]) in alginate matrices cross-linked with polyvalent cations (Ca^{2+} or Fe^{3+}) to prepare the BioSorp Beads. We systematically varied the bead preparation recipe and quantified the outcomes on different bead physical properties (*e.g.*, surface area, pore volume, mechanical strength, swelling, leaching). We also demonstrated that the

3340 | *Environ. Sci.: Water Res. Technol.*, 2024, **10**, 3339–3357

This journal is © The Royal Society of Chemistry 2024

encapsulated microorganisms in the beads remained viable even after an extended storage period (at least 3 months when stored at room temperature) and could disperse from the beads when nutrients were present. Thus, BioSorp Beads hold potential for a variety of multi-media interactions that potentially improve GSI performance.[46]

The specific objective of this research was to quantify BioSorp Bead performance for removal of a suite of representative dissolved stormwater hydrophilic contaminants (one dissolved nutrient and six hydrophilic TOrCs). We selected phosphate (dissolved P nutrient), a neonicotinoid insecticide and its metabolite/transformation product (imidacloprid and desnitro-imidacloprid, respectively), one long-chain PFAS (PFOA), two short-chain PFAS (PFBS and PFBA), and one tire-wear compound (acetanilide) as representative model hydrophilic stormwater runoff relevant compounds to assess the bead contaminant removal performance. Phosphorus (P) is a common stormwater pollutant (from fertilizers, decomposed leaves, pet wastes, *etc.*) that can cause eutrophication in receiving waters.[47] It is well established that 25–50% of total P in stormwater runoff can remain in the dissolved form[47] and dissolved P (>90%) is 3 to 9 times more bioavailable than particulate P (10–30%).[48] Conventional bioretention systems can efficiently remove particulate P; however, dissolved P may pass through the system without being removed.[47] Indeed, some GSI or low impact development systems, such as conventional bioretention cells with high compost amendments to media can even yield a net export of soluble reactive P to receiving water bodies.[49] Thus, modification of traditional GSI systems is necessary for effective dissolved P removal. Neonicotinoid insecticides are commonly used in urban lawns, gardens, indoor planting pots, and for pet treatments and are frequently detected in stormwater.[50–52] Imidacloprid is one of the most common urban-use neonicotinoid insecticides that has high water solubility (610 mg L^{-1} at 20 °C) and lower affinity towards soil particles (log K_{ow} = 0.57).[52–54] Imidacloprid often undergoes a microbial transformation in the environment and produces a metabolite, desnitro-imidacloprid, that is significantly more toxic to mammals (more than 300 times).[52] PFAS such as PFOA, PFBA, and PFBS are extremely environmentally persistent (*i.e.*, 'forever chemicals') and frequently present in stormwater runoff.[21,22] Because BioSorp Beads contain encapsulated sorptive materials and contaminant degrading microorganisms, we hypothesize that the beads can sorb a broad spectrum of TOrCs and dissolved P from urban stormwater runoff and the encapsulated microorganisms can facilitate coupled sorption and fungal biodegradation of stormwater TOrCs.

2. Materials and methods

2.1 Chemicals

Imidacloprid (purity ≥95%), desnitro-imidacloprid hydrobromide (purity ≥95%), and acetanilide (purity ≥99%)

for abiotic and biotic bench-scale experiments were purchased from BOC Sciences, Chem Space, and Acros Organics, respectively. Perfluorooctanoic acid (PFOA) and perfluorobutanoic acid (PFBA) were purchased from Sigma Aldrich. Perfluorobutanesulfonic acid (PFBS) was purchased from Combi-Blocks. Sodium phosphate dibasic was purchased from Research Products International (RPI). Synthetic urban stormwater with common major ions was prepared following our previously described method [Section S1†].[45] Optima LCMS grade solvents (acetonitrile, formic acid, water, methanol) were used for all chromatography analysis. The compositions of different BioSorp Beads are shown in Table S1.†

2.2 Bead performance experimental design

2.2.1 Bead preparation summary. Following our previous approach,[45] we produced BioSorp Beads with encapsulated materials for performance testing [Fig. S2†]. Briefly, in every 50 mL 2% (w/v) sodium alginate solution (made in DI water), we thoroughly mixed 1 g of FeWTR (oven-dried, autoclaved), 1 g of WF (autoclaved), 0.1 g of AQDS, 1 g of PAC (autoclaved), and 50 mL white rot fungi culture (*T. versicolor* or *P. ostreatus*; homogenized; prepared in malt extract broth medium). Then, we slowly added the mixture dropwise onto 270.3 mM CaCl$_2$ or 270.3 mM FeCl$_3$ solution (made in DI water) using a peristaltic pump. Lastly, we air-dried the instantaneously formed composite alginate beads for 2–3 days on wax paper before storing at room temperature. The dried Ca^{2+} alginate beads (diameter: ~2.5 to 3 mm) were spherical in shape, whereas the dried Fe^{3+} alginate beads (~2.5 to 3 mm) exhibited a more spheroidal/disk-like shape. Black carbon (*e.g.*, PAC) can effectively capture a variety of TOrCs and cationic/anionic contaminants onto the different active sorption sites present in the black carbon structure.[31–33] Because iron oxides can capture dissolved phosphorus and PFAS[30,55] and FeWTR is known to contain iron oxides,[35] we included FeWTR in the beads as sorbents and to increase bead density (*i.e.*, avoid medium floating during inundation events). WRF can secrete multiple extracellular (*e.g.*, laccases, lignin peroxidase [LiPs], manganese peroxidase [MnPs]) and intracellular (*e.g.*, CYP450) enzymes and biodegrade various TOrCs, including many recalcitrant compounds.[13,43,56,57] AQDS may aid a variety of biological redox reactions as an electron shuttle[58] and wood flour can act as an energy source/maintenance substrate to increase WRF viability for extended periods.[59] The BioSorp Bead development and characterization are fully described in our recent work.[45]

To investigate the efficacy of BioSorp Beads for removing a wide variety of contaminants from stormwater runoff, we systematically produced different versions of BioSorp Beads and types of synthetic stormwater spiked with dissolved phosphorus and TOrCs (separately) and performed multiple systematic abiotic sorption and sorption–biodegradation experiments. BioSorp Beads (both Ca^{2+} alginate and Fe^{3+}

This journal is © The Royal Society of Chemistry 2024

Environ. Sci.: Water Res. Technol., 2024, **10**, 3339–3357 | **3341**

alginate beads) used in abiotic sorption experiments did not contain any fungi. Multiple varieties of abiotic beads were prepared using different combinations of PAC, WF, FeWTR, and AQDS to investigate the effects of bead materials on contaminant sorption [Tables S1 and S2†]. Conversely, either *T. versicolor* or *P. ostreatus* fungi cultures were encapsulated in Ca^{2+} alginate or Fe^{3+} alginate beads (with and without AQDS; all beads contained PAC, WF, and FeWTR) to produce the BioSorp Beads used in the sorption–biodegradation experiments [Table S3†].

2.2.2 Abiotic sorption experiments. BioSorp Beads with varied compositions were used for abiotic sorption experiments [Table S2†]. These batch-test type experiments were conducted in 125 mL glass serum vials. The crimp-top serum vials were sealed using butyl rubber septa (not lined with PTFE to avoid potential PFAS contributions) and placed inside a dark cardboard box to eliminate potential photoreaction. The box was then maintained on a platform shaker for the duration of the experiment. The vials were periodically removed for sample collection. Analogous experimental and sampling procedures were followed for all experiments.

2.2.2.1 Kinetic experiments for dissolved phosphorus sorption. Sorption kinetic experiments with PO_4^{3-} were conducted by adding 100 mg BioSorp Beads into 100 mL synthetic stormwater solution (pH 7 ± 0.2) spiked with 50 mg L^{-1} PO_4^{3-}. Experiments were conducted using a suite of BioSorp Beads with different compositions. We used the modified Langmuir equation to predict the maximum sorption capacities from the kinetic experiment results for different BioSorp Beads (eqn (1)).

$$q_m = [q_{max}][1 - e^{(-K_{ad})(t)}] \tag{1}$$

where q_m = sorbed concentration at time t (mg g^{-1}), q_{max} = maximum predicted sorption capacity of the sorbent (mg g^{-1}), K_{ad} = adsorption rate constant (1 per day), and t = time (day).

2.2.2.2 Kinetic experiments for tire-wear compound (acetanilide) sorption. We conducted kinetic experiments with PAC and different BioSorp Beads to quantify acetanilide sorption, similar to our lab's prior work.[52] We spiked 100 mL synthetic stormwater with 40 mg L^{-1} acetanilide and added either 100 mg beads or 50 mg PAC as sorbents to measure the sorption values. We used eqn (1) to predict the maximum sorption capacities of PAC and the beads.

2.2.2.3 Kinetic experiments for neonicotinoid sorption. Similar kinetic experiments were conducted with the neonicotinoids. Because imidacloprid contains a nitro group in the structure and desnitro-imidacloprid contains an amine/imine (depending on tautomerization[60]) group in the structure, there are differences in the partial charge distributions of these two neonics.[52] We investigated the interactions of the partial charge distribution differences of the two neonicotinoids and the maximum sorption capacities of the beads (solvent = 100 mL synthetic stormwater spiked

with 30 mg L^{-1} imidacloprid or desnitro-imidacloprid; sorbent = 100 mg BioSorp Beads). The maximum sorption capacities were predicted using eqn (1) (as we had in prior sorption characterization work with neonicotinoids[52]).

2.2.2.4 Isotherm experiments. We developed sorption isotherms with varied concentrations of imidacloprid and desnitro-imidacloprid (10, 15, 20, 25, and 30 mg L^{-1}) for PAC_WF_CaCl$_2$ beads (1% sodium alginate–1% PAC–1% wood flour–3% calcium chloride). Like the kinetic experiments, we added 100 mg beads in 100 mL neonic spiked synthetic stormwater. The maximum imidacloprid and desnitro-imidacloprid sorption capacities were calculated using the following Langmuir equation (eqn (2)):

$$q_e = \frac{(q_{max})(K_L)(C_e)}{1 + (K_L)(C_e)} \tag{2}$$

where q_e = equilibrium sorbed concentration (mg g^{-1}), q_{max} = maximum sorption capacity of the sorbent (mg g^{-1}), K_L = Langmuir constant (L mg^{-1}), and C_e = equilibrium aqueous concentration.

2.2.2.5 Impacts of varied sodium alginate and calcium chloride concentrations, and drying temperatures. We produced multiple types of BioSorp Beads by varying the recipe (varied alginate concentrations [0.5%, 1%, and 1.5% sodium alginate], varying crosslinker concentrations [3% and 5% CaCl$_2$], altering drying temperature [room temperature, 40 °C, 70 °C]) and investigated the impacts of the recipe variations on neonicotinoid sorption kinetics. For these experiments, we added 100 mg beads (sorbents) into 100 mL synthetic stormwater (spiked with 10 mg L^{-1} imidacloprid or desnitro-imidacloprid).

2.2.2.6 Kinetic experiments for PFAS sorption. We designed PFAS sorption kinetic experiments to investigate how the changes in the PFAS carbon chain length (PFOA vs. PFBA—8 carbon vs. 4 carbon) and the PFAS functional groups (PFBA vs. PFBS—carboxylate vs. sulfonate) impact the bead sorption capacities. We used 30 mg BioSorp Beads as sorbents in 200 mL synthetic stormwater (PFAS concentration = 10 mg L^{-1}).

2.2.3 Coupled sorption and biodegradation experiments. We prepared Ca^{2+} alginate beads and Fe^{3+} alginate beads, encapsulating two types of white rot fungi (*T. versicolor* or *P. ostreatus*) to investigate acetanilide removal from synthetic stormwater via fungal treatment beads (BioSorp Beads containing alive white rot fungi), autoclaved control beads (fungi containing BioSorp Beads were autoclaved at 121 °C for 45 minutes), and sodium azide inhibited control beads (10 mM sodium azide were spiked into the synthetic stormwater) [Table S3†]. Azide has previously been shown to inhibit/kill white rot fungi.[13,43,61] We previously demonstrated that *T. versicolor* could biodegrade acetanilide.[13] We added 100 mg beads into every 100 mL acetanilide spiked synthetic stormwater (acetanilide concentration = ~40 mg L^{-1}).

3342 | *Environ. Sci.: Water Res. Technol.,* 2024, **10**, 3339–3357

This journal is © The Royal Society of Chemistry 2024

2.3 Analytical methods, QA/QC and statistical analysis

We quantified imidacloprid and desnitro-imidacloprid concentration using LC-MS/MS (Agilent 1260 Infinity liquid chromatograph and Agilent 6460 triple quadrupole mass spectrometer). We used an Agilent Zorbax eclipse plus C18 column (4.6 mm × 150 mm × 5 μm) with a Zorbax eclipse plus C18 guard column (4.6 mm × 12.5 mm × 5 μm) for the LC-MS/MS analysis. The UIowa High Resolution Mass Spectrometry Facility (https://hrmsf.research.uiowa.edu/) measured our PFAS samples. We measured phosphate concentrations using a Dionex ICS-6000 ion chromatography system. We quantified acetanilide concentrations using a HPLC-DAD [Agilent 1260 liquid chromatography system with diode array detection (DAD)] and a Higgins Analytical Sprite Targa C18 (40 × 2.1 mm, 5 μm) column (including a guard column). Additional details of the analytical methods can be found in the ESI† [Section S2]. If any sample was not analyzed immediately, samples were stored in a refrigerator (at 4 °C) for future analysis. We used GraphPad Prism 9.0.0 (San Diego, CA) for statistical analyses. The Shapiro–Wilk test and normal QQ plot were used to test data distribution normality. If the data were not normally or log-normally distributed, we performed non-parametric analysis (*e.g.*, Mann–Whitney rank sum test). ANOVA ($\alpha = 0.05$) with Tukey *post hoc* tests were used to compare matched-paired datasets.

3. Results and discussion

3.1 Removal of TOrCs and dissolved nutrients *via* abiotic sorption onto BioSorp Beads

3.1.1 Dissolved phosphorus sorption onto BioSorp Beads. Fe^{3+} crosslinked alginate beads were superior at sorbing dissolved phosphorus than Ca^{2+} crosslinked alginate beads (*e.g.*, PAC_WF_WTR_FeCl$_3$ beads [17.03 mg g^{-1}] *vs.*

PAC_WF_WTR_CaCl$_2$ beads [8.25 mg g^{-1}]), with sorption capacity increasing with more available Fe^{3+} ions present in the beads [Fig. 1 and Table S5†]. We observed minimal phosphate sorption onto PAC_WF_CaCl$_2$ beads [0.88 mg g^{-1}] or WF_CaCl$_2$ beads [2.1 mg g^{-1}] (without FeWTR); however, Ca^{2+} alginate beads containing iron water treatment residuals (FeWTR; to simplify the bead names, FeWTR was written as WTR while naming the beads) adsorbed higher amount of phosphate (*e.g.*, WF_WTR_CaCl$_2$ beads [13.01 mg g^{-1}]). Thus, the presence of FeWTR in the Ca^{2+} alginate beads likely contributed to the increased phosphate sorption capacity. Iron water treatment residuals contain different iron oxides and hydroxides that can form strong bonds with phosphate ions.[35,36,62] Due to this phenomenon, iron oxide amended sands (*i.e.*, sand with rusted iron filings) have been previously used to remove dissolved phosphorus from stormwater runoff.[63] Iron shavings (containing amorphous iron oxides) had also been used to remove dissolved phosphorus contaminated runoff.[64] Likewise, Wang *et al.*[37] used ferric alum water treatment residuals (Fe-Al-WTRs) to sorb dissolved phosphorus (maximum sorption capacity = 45.42 mg g^{-1}). Ligand exchange reaction and hydroxide exchange reaction between iron water treatment residuals and phosphate are thought to contribute to the dissolved phase phosphorus sorption.[65] In contrast to our study, Isik *et al.*[66] indicated that Ca^{2+} alginate beads with nothing encapsulated could sorb phosphate up to 3.27 mg g^{-1}.

We note that phosphate removal increased with greater ferric ion quantities available in the beads. The maximum phosphate sorption capacities in WF_WTR_FeCl$_3$ beads and WTR_FeCl$_3$ beads were 42.12 mg g^{-1} and 38.88 mg g^{-1}, respectively. Although we have successfully employed the modified Langmuir kinetic model [eqn (1)] for sorption to black carbon previously,[52] we found this model did not fully
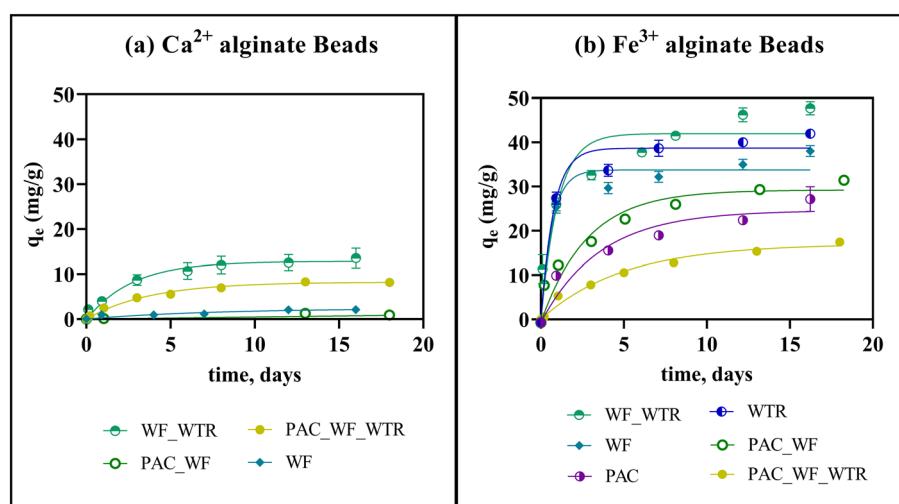

Fig. 1 Phosphate sorption kinetics for different types of alginate beads: (a) Ca-beads and (b) Fe-beads (*n* = 3 experimental replicates; error bars represent standard errors of the means. Some error bars are obscured by the data points as the error bars are small). PAC = powdered activated carbon, WF = wood flour, WTR = iron water treatment residuals. *Sorption capacities were predicted from the modified Langmuir kinetic model [eqn (1)].

This journal is © The Royal Society of Chemistry 2024

Environ. Sci.: Water Res. Technol., 2024, **10**, 3339–3357 | **3343**

match the sorption kinetics for some of the Fe^{3+} crosslinked alginate beads with phosphate (*i.e.*, equilibrium did not appear to be reached for some experimental data), especially in WF_WTR_FeCl$_3$ beads, WTR_FeCl$_3$ beads, and WF_FeCl$_3$ beads. Thus, the actual maximum phosphate sorption capacities of Fe^{3+} alginate beads were potentially higher than eqn (1) results suggested. Because ferric ions in Fe^{3+} crosslinkers can strongly bond with phosphate, Fe^{3+} alginate beads can remove dissolved phosphorus from the aqueous phase.[67] Phosphate removal can also be assisted *via* precipitation (as Fe^{3+}-phosphate salts), which likely results in more phosphate removal than Langmuir adsorption model predicts.[67] Fe^{3+} leached from the bead crosslinkers may form different iron oxides and hydroxides in synthetic stormwater that may also increase phosphate sorption capacities.[63] Iron water treatment residuals in Fe^{3+} alginate beads also exhibited phosphate sorption [*i.e.*, a significantly greater sorption capacity for WF_FeCl$_3$ beads *vs.* WF_WTR_FeCl$_3$ beads (34.03 mg g^{-1} *vs.* 42.12 mg g^{-1}; p = 0.0184)].

3.1.2 Sorption kinetics of acetanilide (tire-wear compound) and imidacloprid/desnitro-imidacloprid (neonicotinoid insecticide/metabolite). The measured surface areas (*via* BET) of the BioSorp Beads were only ~10% of the surface area of raw PAC.[45] Nevertheless, the beads retained more than 50% of the observed acetanilide sorption capacity of raw PAC [Fig. 2], demonstrating high sorption and thus potential for field GSI applications. The observed sorption capacities of raw PAC (surface area = 787.51 m^2 g^{-1}), PAC_WF_CaCl$_2$ beads (surface area = 65.86 m^2 g^{-1}), PAC_WF_WTR_CaCl$_2$ beads (surface area = 45.24 m^2 g^{-1}), and PAC_WF_WTR_FeCl$_3$ beads (surface area = 146.62 m^2 g^{-1}) were 73.77 mg g^{-1}, 39.43 mg g^{-1}, 38.86 mg g^{-1}, and 38.33 mg g^{-1}, respectively. Similar acetanilide sorption ranges were also reported in a recent study with activated carbon (24.7 to 121.2 mg g^{-1}; surface area: 661 to 1031 m^2 g^{-1}).[68] We did not observe any significant difference in sorption capacities for the tested beads (p = 0.8913). When the sorption capacities were normalized with respect to the mass of PAC present in the beads, the PAC-normalized sorption capacities (~135.24 mg g^{-1}) of the beads were ~2 times higher than our observed sorption capacity of raw PAC (73.77 mg g^{-1}). In the context of these kinetic experiment results, our observed acetanilide sorption capacity may be less that the potential maximum sorption capacity of the raw PAC; however, we
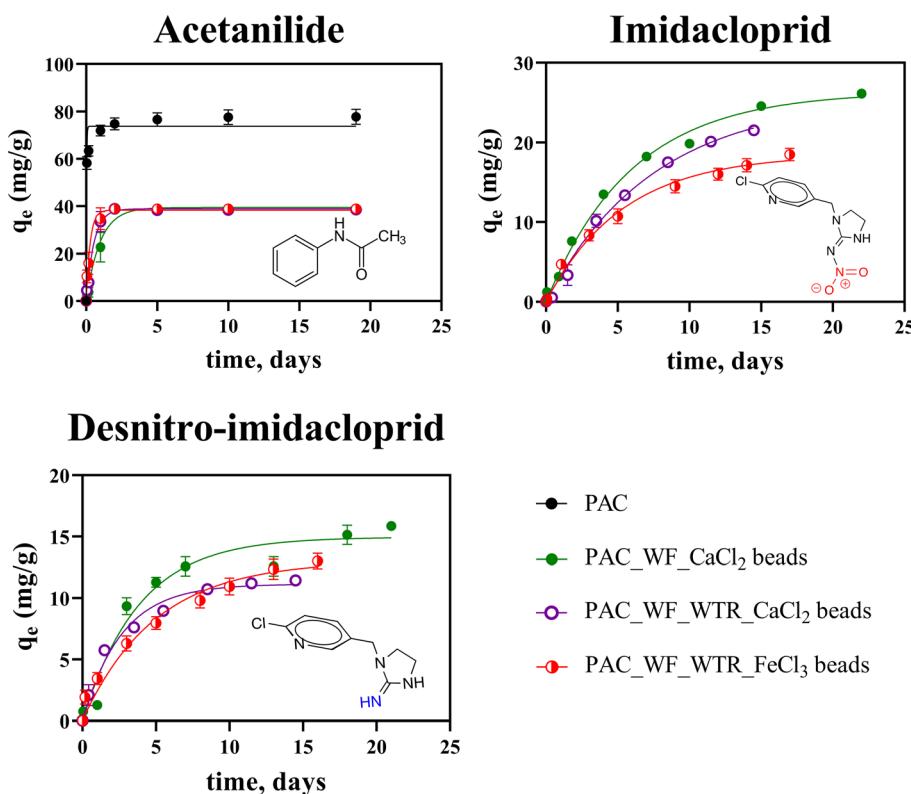
Fig. 2 Acetanilide, imidacloprid, and desnitro-imidacloprid sorption kinetics for different types of BioSorp Beads (n = 3 experimental replicates; error bars represent standard errors of the means. Some error bars are obscured by the data points as the error bars are small). Note different y-axis scales. PAC = powdered activated carbon, WF = wood flour, WTR = iron water treatment residuals, CaCl$_2$ = calcium chloride crosslinker, FeCl$_3$ = ferric chloride crosslinker. *Beads containing no PAC did not significantly sorb the two tested neonicotinoids (p = 0.65) [Fig. S1†]. **Neonicotinoid sorption kinetics of PAC (imidacloprid sorption capacity = 112 mg g^{-1}, desnitro-imidacloprid sorption capacity = 37 mg g^{-1}) can be found in our lab's prior work (Webb *et al.*[52]). Comparison of the maximum sorption capacities of raw PAC and the beads are shown in Fig. 3. ***No acetanilide sorption experiment was performed with beads without PAC. ****Sorption capacities were predicted from modified Langmuir kinetic model [eqn (1)].

3344 | *Environ. Sci.: Water Res. Technol.*, 2024, **10**, 3339–3357

This journal is © The Royal Society of Chemistry 2024

demonstrate here that the PAC present inside the beads could successfully act as an excellent TOrC sorbent even after the sorbents experience alginate encapsulation.

BioSorp Bead compositions affected sorption of the two neonicotinoids, imidacloprid and desnitro-imidacloprid, and the sorption capacities were largely driven by the presence of PAC in the beads [Fig. 2]. The maximum imidacloprid sorption capacities were not different for PAC_WF_CaCl$_2$ beads and PAC_WF_WTR_CaCl$_2$ beads (26.39 mg g^{-1} vs. 25.52 mg g^{-1}; $p >$ 0.9999); however, there was a significant difference between maximum imidacloprid sorption capacities for PAC_WF_WTR_CaCl$_2$ beads vs. PAC_WF_WTR_FeCl$_3$ beads (25.52 mg g^{-1} vs. 18.52 mg g^{-1}; $p = 0.0015$) [eqn (1)]. Conversely, all three types of beads exhibited similar maximum desnitro-imidacloprid sorption (PAC_WF_CaCl$_2$ beads [14.96 mg g^{-1}] vs. PAC_WF_WTR_CaCl$_2$ beads [11.14 mg g^{-1}]; $p = 0.14$; PAC_WF_WTR_CaCl$_2$ beads [11.14 mg g^{-1}] vs.

PAC_WF_WTR_FeCl$_3$ beads [13.04 mg g^{-1}]; $p = 0.73$). The beads in which we encapsulated only wood flour and iron water treatment residuals did not sorb imidacloprid or desnitro-imidacloprid [Fig. S1†]. This result demonstrates that neonicotinoid sorption to the BioSorp Beads is driven by PAC presence in the beads. We previously reported high imidacloprid and desnitro-imidacloprid sorption onto GAC, PAC, and carbon nanotubes (CNTs) in our lab's previous studies.[52,69] Black carbons have multiple active adsorption sites consisting of single and double carbon bonds, hydroxyl groups, metal oxides and hydroxides, aldehyde groups, carboxyl groups, aromatic carbon skeletons with delocalized pi electrons, and other oxygen-rich functional groups.[70,71] As a result, black carbon, such as PAC, can effectively sorb various trace organics and ionic contaminants.

Imidacloprid contains a strongly electron-withdrawing nitro group, which results in a negative partial charge
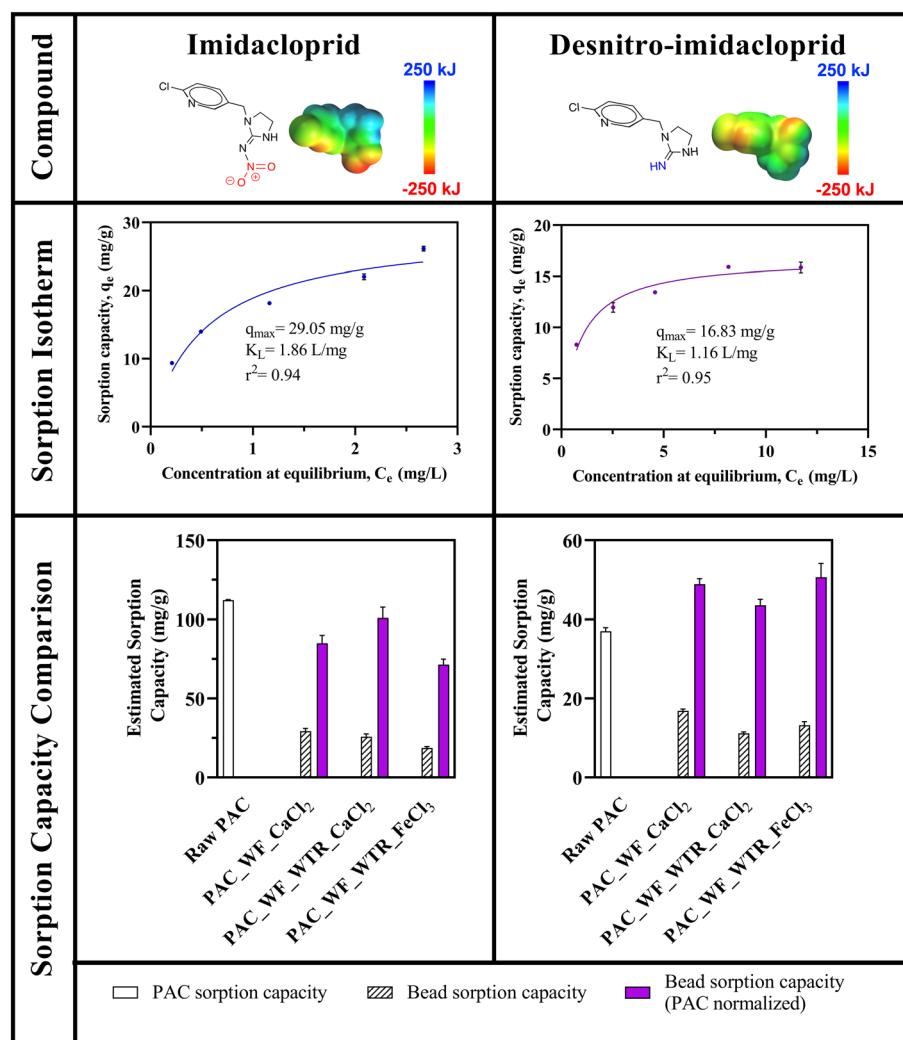
Fig. 3 Imidacloprid and desnitro-imidacloprid sorption isotherms for PAC_WF_CaCl$_2$ beads and comparisons of maximum neonicotinoid sorption capacities for different BioSorp Beads and the maximum sorption capacities when normalized to the amount of PAC present in the beads ($n = 3$ experimental replicates; error bars represent standard errors of the means. Some error bars are obscured by the data points as the error bars are small). ***Sorption isotherm data were fitted using the Langmuir equation [eqn (2)]. **Sorption capacities were predicted from a modified Langmuir kinetic model [eqn (1)]. *PAC maximum sorption capacities are from our lab's prior work (Webb et al.[52]).

This journal is © The Royal Society of Chemistry 2024

Environ. Sci.: Water Res. Technol., 2024, **10**, 3339–3357 | **3345**

distribution of the molecule due to the insecticidal pharmacophore (*i.e.*, functional group that imparts biological activity).[52] Conversely, desnitro-imidacloprid contains an electron-donating amine/imine (depending on tautomerization[60]) group, which yields a net positive partial charge distribution.[52] Because alginate gel contains a high number of negatively charged hydroxyl and carboxyl groups (alginic acid $pK_a = 3$), we decided to further probe neonicotinoid sorption mechanisms and possible interactions with compound partial charge distributions and BioSorp Bead sorption capacities.

3.1.3 Neonicotinoid adsorption to probe partial charge electrostatic interactions. The presence of black carbon (PAC) was crucial for neonicotinoid sorption onto BioSorp Beads and sorption was not achieved with the beads that did not contain black carbon materials [Fig. 3 and S1†]. Neonicotinoid sorption increased with greater amounts of PAC present in the beads. From our isotherm experiments, we observed that PAC_WF_CaCl$_2$ beads could sorb up to 29.05 mg g^{-1} imidacloprid and up to 16.83 mg g^{-1} desnitro-imidacloprid [eqn (2)]. The predicted maximum imidacloprid and desnitro-imidacloprid sorption capacities of PAC_WF_WTR_CaCl$_2$ beads were 25.52 mg g^{-1} and 11.14 mg g^{-1}, respectively [eqn (1)]. PAC_WF_WTR_FeCl$_3$ beads exhibited a maximum imidacloprid sorption capacity of 18.52 mg g^{-1} and a maximum desnitro-imidacloprid sorption capacity of 13.04 mg g^{-1}. We also normalized the bead sorption capacities with respect to the mass of PAC present in the beads to compare the surface area and sorption capacity values among BioSorp Beads (both Ca^{2+} alginate beads and Fe^{3+} alginate beads) and raw PAC (*i.e.*, unencapsulated PAC). The average decrease in imidacloprid sorption capacity values (PAC-normalized; $p = 0.0272$) of the beads was ~3.7 times less than the average decrease in bead surface area[45] (~24% *vs.* ~89% decrease, respectively) [Fig. 3]. Because some of the sorption sites present on the PAC surface likely were blocked during encapsulation, sorption capacities for imidacloprid were lower than for unencapsulated PAC. Interestingly, we discovered that the average PAC-normalized desnitro-imidacloprid sorption capacity onto BioSorp Beads was even greater than raw PAC's sorption capacity (increased by ~19%; $p = 0.0327$) [Fig. 3]. Additionally, the sorption rate constant of desnitro-imidacloprid was 1.75 times higher than that of imidacloprid (average 0.28 per day *vs.* 0.16 per day) [Fig. 2]. We postulate that differences in imidacloprid and desnitro-imidacloprid partial charge distributions led to the opposing sorption effects, as detailed below.

3.1.4 Effects of compound partial charge distributions on BioSorp Bead sorption capacities. The partial charge distributions of imidacloprid and desnitro-imidacloprid likely impacted the maximum neonicotinoid sorption onto the BioSorp Beads. When the maximum neonicotinoid sorption capacities of the beads are normalized to the mass of raw PAC present in the recipes, we observed that PAC-normalized imidacloprid sorption capacity in PAC_WF_CaCl$_2$ beads,

PAC_WF_WTR_CaCl$_2$ beads, and PAC_WF_WTR_FeCl$_3$ beads respectively decreased by ~25%, ~11%, and ~37% compared to raw PAC's capacity [Fig. 3]. Conversely, desnitro-imidacloprid sorption capacity (PAC-normalized) respectively increased by ~22%, ~9%, and ~25% in PAC_WF_CaCl$_2$ beads, PAC_WF_WTR_CaCl$_2$ beads, and PAC_WF_WTR_FeCl$_3$ beads when compared with raw PAC's sorption capacity [Fig. 3].

The differences in observed sorption effects were likely due to the electrostatic interactions between alginate and the electronegative functional group on imidacloprid *versus* the electron-donating group of desnitro-imidacloprid. Our lab previously reported these types of electrostatically driven interactions for imidacloprid and desnitro-imidacloprid sorption onto granular activated carbon (GAC) and carbon nanotubes (CNTs).[52] GAC contains many localized charges with basic functional groups and favors imidacloprid sorption over desnitro-imidacloprid sorption at circumneutral pH.[52] Furthermore, the evidence for the effects of partial charge distributions on neonicotinoid sorption was bolstered by past neonicotinoid sorption isotherms that were generated for functionalized and non-functionalized CNTs. Specifically, carboxylic acid functionalized CNTs exhibited greater sorption capacity for desnitro-imidacloprid than amine functionalized CNTs. The opposite effect occurred for imidacloprid sorption, where amine functionalized CNTs sorbed more imidacloprid than carboxylic acid functionalized CNTs. At neutral pH, the carboxylate group is negatively charged and imidacloprid can act as a hydrogen bond acceptor ($pK_a < 5$), whereas the amine group is positively charged and desnitro-imidacloprid can work as a hydrogen bond donor. Consequently, the presence of higher amounts of carboxylate groups on the CNTs increased desnitro-imidacloprid sorption, whereas the sorption was inhibited in the presence of higher amounts of amine groups on the CNTs. Alginate gel contains abundant quantities of negatively charged hydroxyl and carboxyl groups at neutral pH (pK_a of alginic acid is 3), which can be crosslinked with positively charged Ca^{2+} or Fe^{3+} ions.[72–74] These abundant deprotonated groups present on the alginate structures may yield some attractive forces with the electron-donating amine/imine (depending on tautomerization[60]) group present on desnitro-imidacloprid, increasing the sorption capacity. Indeed, desnitro-imidacloprid is a concerning contaminant metabolite due to its higher toxicity towards mammals (~300 times more toxic)[75] and BioSorp Beads could improve desnitro-imidacloprid sorption in engineered bioretention systems. In contrast, activated carbon alone exhibits superior removal of imidacloprid over desnitro-imidacloprid.

For all three types of beads tested, there were significant differences between imidacloprid and desnitro-imidacloprid sorption capacities (PAC_WF_CaCl$_2$ beads [$p < 0.0001$], PAC_WF_WTR_CaCl$_2$ beads [$p < 0.0001$], and PAC_WF_WTR_FeCl$_3$ beads [$p = 0.0191$]). Because PAC_WF_CaCl$_2$ beads are less dense than PAC_WF_WTR_CaCl$_2$ beads due to the absence of the iron water treatment residuals, PAC_WF_CaCl$_2$

3346 | *Environ. Sci.: Water Res. Technol.*, 2024, **10**, 3339–3357

This journal is © The Royal Society of Chemistry 2024

beads consequently contain a greater mass of alginate and concomitantly more negatively charged ions than PAC_WF_WTR_CaCl$_2$ beads for the same total bead mass. As a result, although PAC_WF_CaCl$_2$ beads contained more PAC inside per bead than PAC_WF_WTR_CaCl$_2$ beads, PAC_WF_CaCl$_2$ beads resulted in lower PAC-normalized imidacloprid sorption than PAC_WF_WTR_CaCl$_2$ beads [Fig. 3]. This is further evidence of the electrostatically impacted neonicotinoid sorption of the beads. Trivalent iron produces denser and stronger crosslinks with alginate than divalent calcium, which likely hindered contaminant diffusion through the alginate crosslinks.[76,77] Additionally, Fe^{3+} bonds with both polyguluronate (GG) and polymannuronate (GM) groups of alginates in Fe^{3+} alginate beads, whereas Ca^{2+} bonds only with polyguluronate (GG) groups of alginates in Ca^{2+} alginate beads.[77] As a result, Fe^{3+} alginate beads likely contain more negatively charged surface groups (due to the higher number of carboxylic ions present), which could explain the increases in desnitro-imidacloprid sorption. Similar alginate interactions between partial charges were also reported in a previous study, where the release of cationic drugs from alginate bead system was slower than the release of anionic drugs.[78]

Varying alginate concentration or crosslinker concentration in the bead recipe impacted neonicotinoid sorption kinetics, whereas bead drying temperature did not have any effect on the sorption rates [Fig. 4]. With increasing sodium alginate and/or calcium chloride concentrations in

the recipe, denser crosslinked structures were formed.[45] It is likely that contaminant diffusion through the beads becomes slower in denser structures. We observed this same pattern in our neonicotinoid sorption kinetic experiments. When we increased the alginate and/or crosslinker concentrations in the bead production recipe, the first-order loss rates decreased for both neonicotinoids [Table S4†]. When the sodium alginate concentration was increased to 1.5% from 0.5%, the imidacloprid sorption rate became 0.13 per day from 0.22 per day and desnitro-imidacloprid sorption rate became 0.17 per day from 0.21 per day. When the calcium chloride concentration was raised to 5% from 3%, both imidacloprid sorption rate (became 0.16 per day from 0.19 per day) and desnitro-imidacloprid sorption rate decreased (became 0.15 per day from 0.18 per day). We did not observe any impact of bead drying temperatures on the neonic sorption kinetics (p = 0.1592). We tested three kinds of BioSorp Beads with varied drying temperature (beads dried at room temperature, beads dried at 40 °C, and beads dried at 70 °C) and did not observe any significant differences in neonicotinoid sorption rates [imidacloprid (p = 0.2921), desnitro-imidacloprid (p = 0.6131)].

3.1.5 PFAS sorption onto BioSorp Beads. BioSorp Beads adsorbed a greater mass of long-chain PFAS (PFOA) than short-chain PFAS (PFBA and PFBS) from synthetic stormwater runoff [Fig. 5]. Most of our PAC-free Ca^{2+} alginate beads did
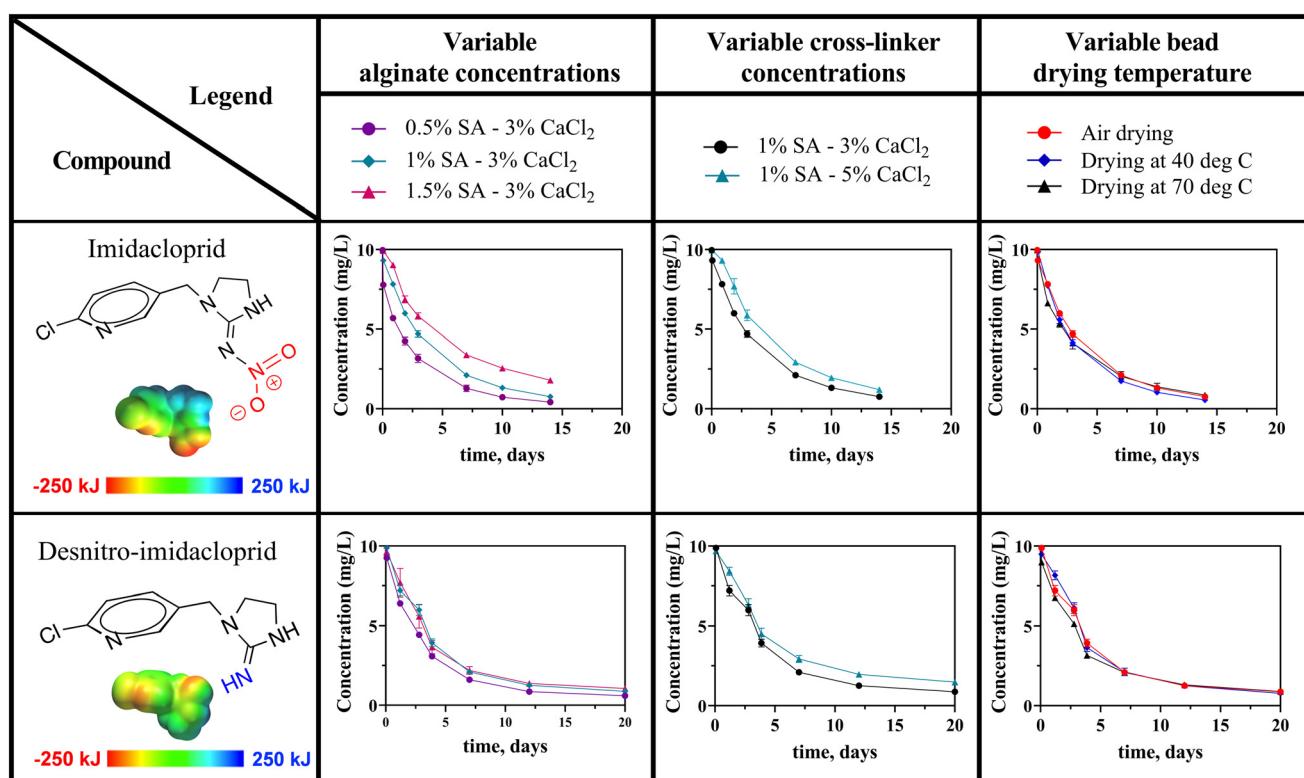

Fig. 4 Effects of varied alginate concentration, varied crosslinker (calcium chloride) concentration, and varied drying temperature of different BioSorp Beads on imidacloprid and desnitro-imidacloprid sorption kinetics (n = 3 experimental replicates; error bars represent standard errors of the means. Some error bars are obscured by the data points as the error bars are small). SA = sodium alginate, CaCl$_2$ = calcium chloride crosslinker.

This journal is © The Royal Society of Chemistry 2024

*Environ. Sci.: Water Res. Technol.*, 2024, **10**, 3339–3357 | **3347**
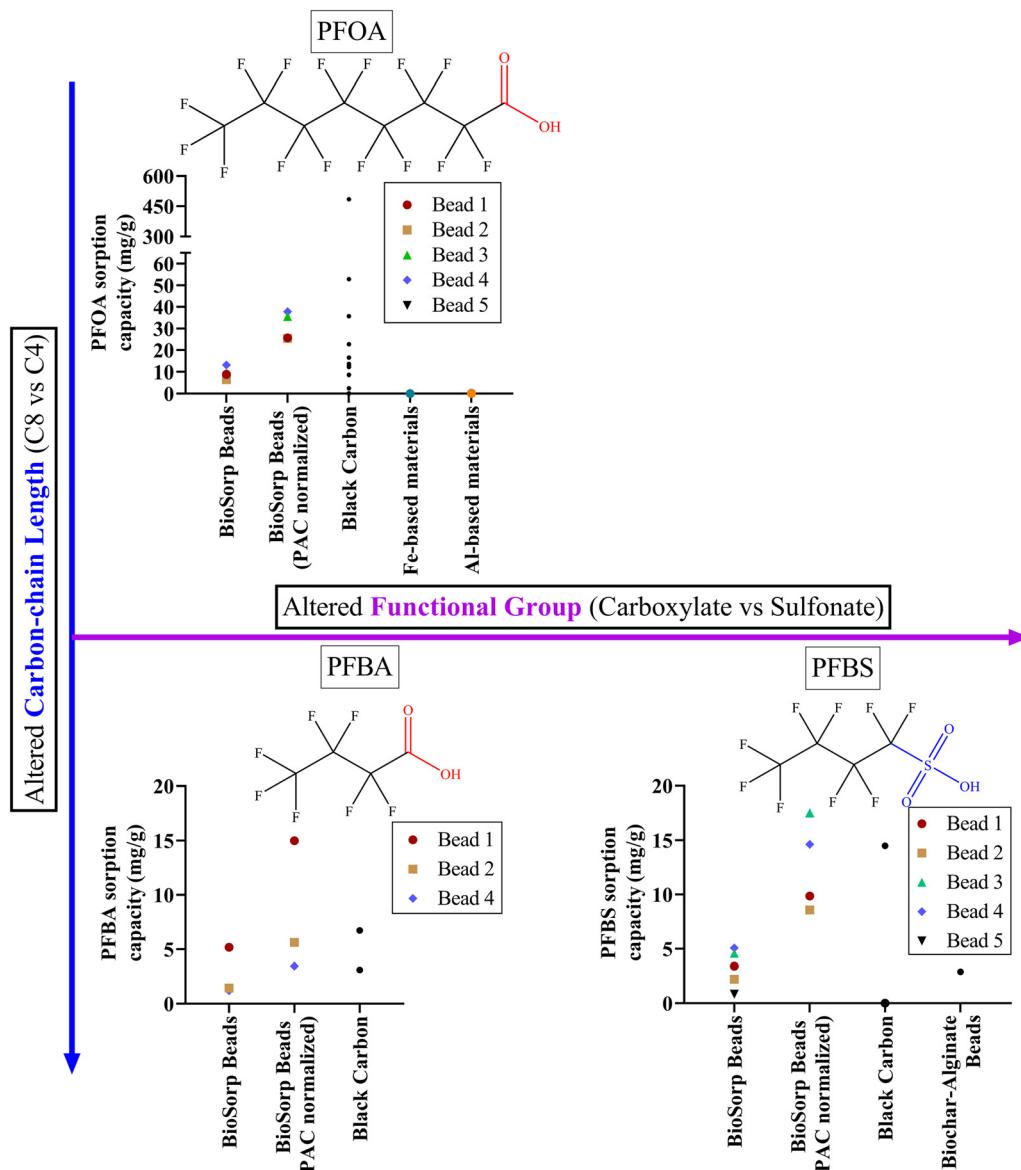
Fig. 5 Comparison of three different PFAS sorption onto different BioSorp Beads and other common sorptive materials found in the literature. The sorption capacity values and the references can be found in Table S6† [bead compositions: bead 1: 1% sodium alginate–1% PAC (powered activated carbon)–1% wood flour–3% $CaCl_2$, bead 2: 1% sodium alginate–1% PAC–1% wood flour–1% FeWTR–3% $CaCl_2$, bead 3: 1% sodium alginate–1% wood flour–1% FeWTR–3% $CaCl_2$, bead 4: 1% sodium alginate–1% PAC–1% wood flour–1% FeWTR–270.3 mM $FeCl_3$, bead 5: 1% sodium alginate–1% wood flour–1% FeWTR–270.3 mM $FeCl_3$].

not sorb any PFAS (the only exception was the WF_WTR_$CaCl_2$ beads; sorbed 0.4 mg PFBS per g of beads). This indicates that PFAS sorption was dominated by sorption onto the PAC present in the Ca^{2+} alginate beads. Black carbon materials such as PAC can effectively sorb long-chain PFAS *via* hydrophobic interactions, whereas short-chain PFAS removal is driven by electrostatic interactions.[30] Conversely, we observed 6.9 mg PFOA per g and 0.9 mg PFBS per g sorption onto PAC-free Fe^{3+} alginate beads. This demonstrates that the Fe^{3+} ions in the bead crosslinkers facilitated PFOA sorption. Ahn *et al.*[79] soaked granular activated carbon in $FeCl_3$ solution and similarly observed an increase in PFOA sorption due to the presence of Fe^{3+} ions.

Additionally, Fe^{3+} ions can also leach from the bead crosslinker and precipitate as different iron oxides and hydroxides.[45] Metal oxides and hydroxides can sorb PFAS *via* electrostatic interactions, ligand exchange with –COO^- or –SO_3^- groups present in PFAS structures (at environmentally relevant pH conditions), hydrophobic interactions, and hydrogen bonds.[30,80] When we added FeWTR in the recipe, we observed a decrease in all three PFAS sorption in both Ca^{2+} alginate and Fe^{3+} alginate beads. Nevertheless, this phenomenon is attributable to the lower mass of black carbon in the beads containing FeWTR (*i.e.*, total PAC mass displaced for the same total mass of bead). When we consider the mass of PAC present in the beads, we observed

similar PAC normalized sorption capacity values in with *vs.* without FeWTR beads [(PFOA—PAC_WF_CaCl$_2$ beads *vs.* PAC_WF_WTR_CaCl$_2$ beads: 25.7 mg g^{-1} *vs.* 25.4 mg g^{-1}; PAC_WF_FeCl$_3$ beads *vs.* PAC_WF_WTR_FeCl$_3$ beads: 37.8 mg g^{-1} *vs.* 35.5 mg g^{-1}); (PFBS—PAC_WF_CaCl$_2$ beads *vs.* PAC_WF_WTR_CaCl$_2$ beads: 9.9 mg g^{-1} *vs.* 8.6 mg g^{-1} and PAC_WF_FeCl$_3$ beads *vs.* PAC_WF_WTR_FeCl$_3$ beads: 14.6 mg g^{-1} *vs.* 17.5 mg g^{-1})] (exception: PFBA sorption) [Table S6†]. The FeWTR in the beads could also partially contribute to PFAS sorption because FeWTR can contain many amorphous iron oxides and/or hydroxides.[35,36] For example, Zhang *et al.*[81] used aluminum-based water treatment residuals (comparable to FeWTR; contains amorphous metal oxide and/or hydroxides) for PFOA removal and reported a maximum sorption capacity of ~0.1 mg g^{-1} (at neutral pH). Similarly, Ordonez *et al.*[82] used an iron filings-based medium (contains sand, recycled zero-valent iron, and clay) and sorbed up to 7 × 10^{-9} mg g^{-1} PFOA.

For the majority of the BioSorp Beads we tested, sorption removal was greater for PFBS than for PFBA (exception: sorption onto PAC_WF_CaCl$_2$ beads—5.2 mg PFBA per g

beads *vs.* 3.4 mg PFBS per g beads). It is well documented in the literature that PFBS sorption onto black carbon is greater than PFBA sorption (*i.e.*, sulfonate *vs.* carboxylate C-4 PFAS compounds), likely due to the higher hydrophobic interactions between PFBS and the sorbents[30]—PFBS has lower water solubility (46.2 g L^{-1}) than PFBA (214 g L^{-1}).[83,84] The log K_{ow} values of PFOA, PFBA, and PFBS were reported as 4.59, 2.32, and 2.73, respectively.[85] Additionally, based on Pearson's soft/hard acid/base theory, the sulfonate group in PFBS acts as a hard base, whereas the carboxylate group in PFBA works as a soft base; the hard base preferentially interacts with the hard acid.[86,87] The higher PFBS removal was also likely attributed to the interactions between iron oxides (which can also work as a hard acid) and PFBS.[86,87] As described, iron oxides could exist either on the FeWTR structures or could be generated in synthetic stormwater by the leached Fe^{3+} from crosslinkers. Additionally, the oxygen atoms in the PFBS sulfonate groups are more electronegative than the oxygen atoms in PFBA carboxylate groups (based on density functional theory).[88] Finally, the Fe^{3+} alginate beads (equilibrium pH of DI water containing Fe^{3+} alginate beads
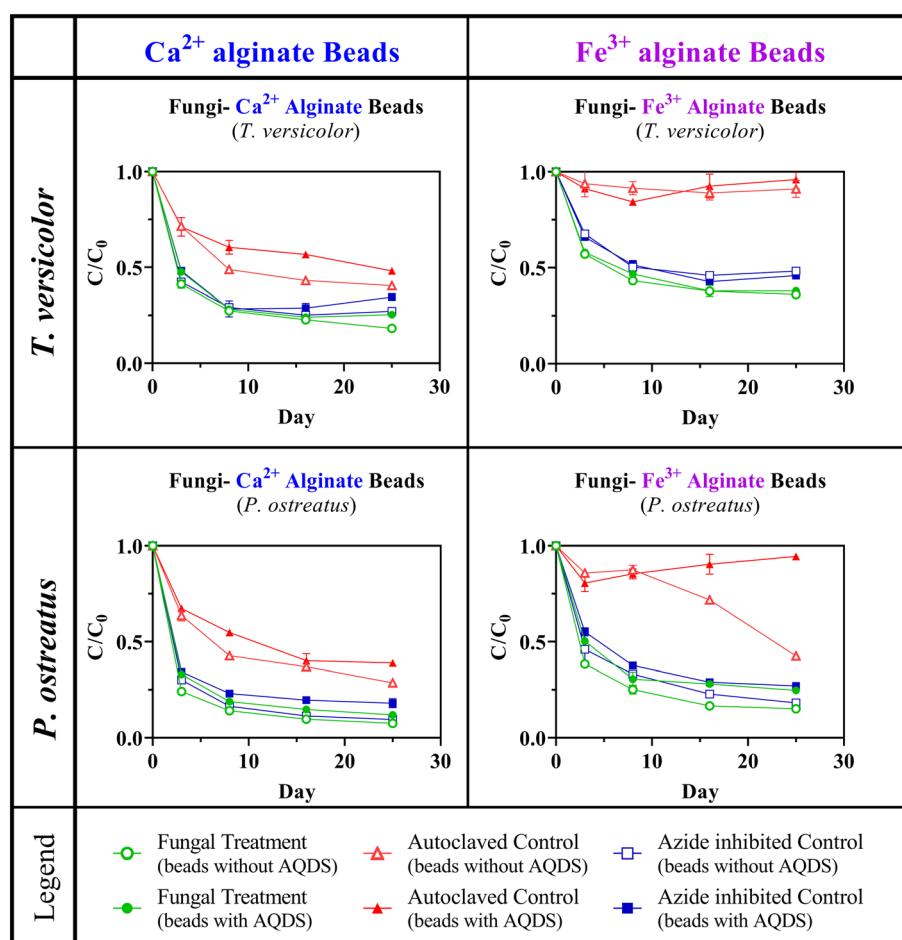
Fig. 6 Coupled sorption and biodegradation of acetanilide *via* BioSorp Beads (different types of composite Ca^{2+} alginate and Fe^{3+} alginate beads) [initial acetanilide concentration = ~40 mg L^{-1}] (*n* = 3 experimental replicates. Error bars represent standard errors of the means. Fungi species encapsulated were *T. versicolor* and *P. ostreatus*. Some error bars are obscured by the data points as the error bars are small). AQDS (anthraquinone-2,6-disulfonate) is a model electron shuttling compound.

This journal is © The Royal Society of Chemistry 2024

Environ. Sci.: Water Res. Technol., 2024, **10**, 3339–3357 | **3349**

was ~3.5) had lower pH than PAC (pH_{PZC} ~7).[89] As such, the PAC inside the Fe^{3+} alginate beads may be more positive than the PAC inside Ca^{2+} alginate beads (equilibrium pH of DI water containing Ca^{2+} alginate beads was ~6.5). As a result, Fe^{3+} alginate beads likely sorbed more PFBS than Ca^{2+} alginate beads. PFBS sorption capacities in PAC_WF_$CaCl_2$ and PAC_WF_$FeCl_3$ beads were 3.4 mg g^{-1} and 5.1 mg g^{-1}, respectively. PFBS sorption capacities in PAC_WF_WTR_$CaCl_2$ and PAC_WF_WTR_$FeCl_3$ beads were 2.2 mg g^{-1} and 4.6 mg g^{-1}, respectively. A combination of the aforementioned mechanistic factors likely contributed to the enhanced sorption of PFBS (containing a sulfonate group) to the beads compared to PFBA (containing a carboxylate group).

3.2 Demonstrating coupled sorption and fungal degradation *via* BioSorp Beads

We observed the greatest total acetanilide (as a representative TOrC) removal in the fungal treatment beads and the lowest removal in autoclaved control beads (for both Ca^{2+} alginate and Fe^{3+} alginate beads; two types of white rot fungi were encapsulated), yielding strong evidence of coupled contaminant sorption and biodegradation. Ca^{2+} alginate beads containing live fungi (treatment beads) removed 1.3 to 1.6 times more acetanilide than autoclaved fungi–Ca^{2+} alginate beads, whereas Fe^{3+} alginate beads containing live fungi (treatment beads) removed 1.3 to 15.7 times more acetanilide than autoclaved fungi–Fe^{3+} alginate beads [Fig. 6]. This phenomenon provides strong proof-of-concept evidence of TOrC biodegradation (*i.e.*, TOrC removal beyond sorption). We hypothesize that the autoclaved fungi beads most closely represented abiotic conditions (because most, if not all, of the encapsulated fungi were dead/severely inhibited). Importantly, we did not observe any fungal growth from the autoclaved fungi beads when the beads were maintained in malt extract medium. Beads that did not contain any fungi [Fig. 2] sorbed a higher amount of acetanilide than the autoclaved fungi–Ca^{2+}/Fe^{3+} alginate beads [Fig. 6]. We presume that fungal biofilms blocked some of the bead sorption sites on the beads.

Because contaminant biodegradation is crucial for sustained stormwater treatment and biodegradation can renew bioretention sorption capacities,[42] BioSorp Beads containing viable microorganisms are the intended long-term vision for field deployment in GSI systems. Importantly, we discovered that alginate encapsulation appeared to protect the fungi from harsh conditions, which could thus increase bioaugmentation success potential. Sodium azide is regularly used for microbial inhibition and was also successfully utilized in previous studies with white rot fungi.[13,43,61] Nevertheless, acetanilide removal in our azide-inhibited control beads was not significantly different from the removals in our fungal treatment beads ($p = 0.3583$). This phenomenon indicates that the encapsulated fungi were alive and actively biodegrading acetanilide even after we spiked

sodium azide into the synthetic stormwater. Although the addition of sodium azide for microbial inhibition does not represent a condition to which organisms would be exposed in the field bioretention cells, the demonstrated robustness of the encapsulated organisms to a harsh condition in the laboratory (*i.e.*, azide exposure) indicates that the beads may be able to improve microbial viability and resilience under variable environmental conditions (*e.g.*, exposure to a toxicant). Indeed, encapsulated microorganisms tend to be more viable, stable, and active.[90] Hence, we infer that our bioactive composite alginate bead geomedia could help the encapsulated microorganisms to remain viable and active in field bioretention conditions even under unfavorable environmental conditions.

Inclusion of AQDS in the beads impacted total acetanilide removal; however, the effects varied from bead type to type. Because electron shuttles (AQDS was used as a model electron shuttle) can facilitate various microbial redox reactions as well as recalcitrant contaminant degradation,[45] inclusion of some type of electron shuttling compounds in the bead recipe is expected to provide long-term biodegradation benefits (quantifying these values is an area of future research). At the end of the experiments, *P. ostreatus*—Ca^{2+} alginate beads were not likely affected by AQDS (89% removal [with] *vs.* 92% removal [without]; initial acetanilide concentration = ~40 mg L^{-1}; $p = 0.0547$) but acetanilide removal was marginally lower in *T. versicolor*—Ca^{2+} alginate beads when AQDS was present (75% removal [with] *vs.* 82% removal [without]; initial acetanilide concentration = ~40 mg L^{-1}; $p = 0.0376$). Conversely, AQDS did not have any impact on *T. versicolor*—Fe^{3+} alginate beads (64% removal [with] *vs.* 63% removal [without]; initial acetanilide concentration = ~40 mg L^{-1}; $p = 0.7599$) but acetanilide removal decreased in *P. ostreatus*—Fe^{3+} alginate beads when AQDS was present (75% removal [with] *vs.* 85% removal [without]; initial acetanilide concentration = ~40 mg L^{-1}; $p = 0.0229$). This small decrease in acetanilide removal may relate to the slight decrease in bead surface area when AQDS is present (*i.e.*, blocking some of the sorption sites).[45] We deliberately used high initial acetanilide concentration in these experiments that we recognize are not likely environmentally relevant for stormwater with the goal of demonstrating proof-of-concept coupled sorption and biodegradation. Using a lower concentration would likely lead to complete sorption of the acetanilide and would thus make distinguishing between sorption and biodegradation tenuous.

3.3 Summary of findings and environmental implementation potential

Because GSI is typically designed with short hydraulic retention times to mitigate flooding *via* infiltration, amending GSI with sorptive materials can potentially improve remove of stormwater relevant contaminants. In this work, we experimentally demonstrated that the sorbent

3350 | *Environ. Sci.: Water Res. Technol.*, 2024, **10**, 3339–3357

This journal is © The Royal Society of Chemistry 2024

materials (PAC and FeWTR) encapsulated in BioSorp Beads could capture different TOrCs. We also observed that FeWTR and Fe^{3+} crosslinker played important roles in capturing phosphate and (to some extent) PFAS. Along with the crosslinker, the negatively charged surface groups in alginate also impacted TOrC sorption. For instance, Fe^{3+} alginate beads sorbed more desnitro-imidacloprid (contains an electron-donating group) and less imidacloprid (contains an electron-accepting group) than Ca^{2+} alginate beads likely because Fe^{3+} crosslinker hosts more negatively charged alginate groups than Ca^{2+} crosslinker. We also found evidence of combined bead TOrC sorption and biodegradation (using acetanilide), indicating potential for sustained TOrC removal and *in situ* GSI renewal. Urban stormwater typically contains a wide variety of TOrCs; biodegradation can often generate less environmentally harmful degradation products for many contaminants.[91] The diverse microbial communities in GSI could potentially work synergistically to produce benign transformation products; for example, fungi might initiate the degradation of a recalcitrant contaminant, which could be further degraded into harmless metabolites by diverse soil bacteria.[92–94] Nevertheless, it is important to recognize that some TOrC degradation products can be more toxic than the parent compound (*e.g.*, desnitro-imidacloprid is more toxic for mammals than parent imidacloprid) or more mobile/recalcitrant. Thus, we posit that coupled contaminant sorption and biodegradation in GSI would likely generate overall environmental benefits, but that it is important to be mindful of the full fate pathways of contaminants.

In addition to facilitating contaminant biodegradation, bioaugmentation with white rot fungi may also affect GSI plant diversity and growth by producing various intra- and extracellular enzymes. Bioretention cells generally host diverse types of fungi (including the groups that include white or brown rot fungi) and fungal diversity correlates to the bioretention cell plant types.[44] Selecting plant species that host and/or favor white rot fungi may improve plant growth in white rot fungi augmented bioretention cells. Bioaugmentation with other fungal species could improve plant growth; Palacios *et al.*[95] inoculated stormwater biofilters with mycorrhizal fungi to increase bioretention, plant growth and drought tolerance. BioSorp Beads adaptively prepared with encapsulated mycorrhizal fungi could be deployed (during or post construction phase) in bioretention cells to stimulate the plant growth.

The work presented to date was focused on development and testing of BioSorp Beads, but considering challenges of scaling is useful for future environmental implementation efforts. Due to the adaptability of the recipe and the low-cost raw materials, industrial scaling of bead production should be straightforward and economical (*e.g.*, larger container, mixer, pump, drying area are required). For example, ferric sludge as water treatment residual is a valorized waste product and incorporation into BioSorp Beads represents a beneficial reuse. Drying ferric sludge to produce FeWTR, properly autoclaving raw materials, and drying the freshly prepared beads may represent the most challenging scaling steps in the production process. Although we observed no difference in fungal viability after storing the beads at room temperature for three months,[45] we recommend storing the beads at 4 °C (when produced in larger scale) instead of storing at room temperature to increase the likely bead shelf life[59] (which would increase production cost).

4. Conclusions

The objective of this research was to determine our recently developed BioSorp Bead's potential to remove a variety of urban stormwater relevant dissolved trace organic contaminants and dissolved phosphorus. We reveal that the beads are capable of effectively capturing dissolved P and TOrCs as well as a proof-of-concept demonstration of coupled sorption/biodegradation of a selected TOrC. In our previous work, we described the development and characterization processes of BioSorp Beads, proved that encapsulated microorganisms remained viable in dried beads even after a prolonged storage period and could also spread from the beads, indicating potential to bioaugment green stormwater infrastructure.[45] In the work presented here, we used two types of white rot fungi (*T. versicolor* and *P. ostreatus*) as model contaminant degrading microorganisms to demonstrate dissolved TOrC biodegradation. Although we encapsulated powdered activated carbon and iron water treatment residuals as sorbents and white rot fungi as the biodegrading organisms, the BioSorp Beads could easily be adapted and prepared using other contaminant-specific degrading microorganisms, maintenance substrates, or sorbents needed for a range of desired applications.

BioSorp Bead are thus highly robust and customizable, with potential applications beyond TOrC removal from urban stormwater runoff in GSI.[45] For example, BioSorp Beads could be produced encapsulating a wide variety of biodegrading microorganisms, such as anammox bacteria,[96] nitrifying/denitrifying bacteria,[97] PCB degrading bacteria,[98] or Feammox bacteria[99] (*e.g.*, low pH conditions in Fe^{3+} alginate beads could potentially sustain the acidophilic PFAS-degrading bacteria). Similarly, beads could also likely be prepared with different sorbents to exploit specific interactions with contaminants, supporting nutrients, and/or electron shuttles such as powdered biochar[31] (sorbent), functionalized carbon nanotubes[52] (sorbent), graphene oxide powder[100] (sorbent), iron oxide nanoparticles[101] (sorbent), clay-modified with zinc oxide[102] (sorbent), aluminum water treatment residuals[103] (sorbent), rice husks[96] (maintenance substrate), shredded newspaper[104] (maintenance substrate), shredded straw[105] (maintenance substrate), microbial/plant/artificial root exudates[106–109] (electron shuttle), *etc.* We posit

This journal is © The Royal Society of Chemistry 2024

Environ. Sci.: Water Res. Technol., 2024, **10**, 3339–3357 | **3351**

that BioSorp Beads hold the potential to improve contaminant sorption during storm events and subsequent biodegradation to thereby decouple the longer contaminant residence time needed for achieving biodegradation from the short hydraulic residence time due to fast infiltration rates required in GSI.[45] Biodegradation could increase GSI service life and decrease maintenance needs by renewing GSI sorption capacity *in situ*.[42] BioSorp Beads also could act as a vehicle for bioaugmenting beneficial biodegrading microbes into existing GSI systems. Thus, modifying existing and/or future GSI with BioSorp Beads could provide a long-term sustainable stormwater management, ultimately resulting in improved water quality.

Data availability

The data supporting this article have been included as part of the ESI.†

Author contributions

Debojit S. Tanmoy: conceptualization, methodology, software, formal analysis, investigation, data curation, writing – original draft, visualization, project administration. Gregory H. LeFevre: conceptualization, methodology, resources, writing – review & editing, supervision, visualization, project administration, funding acquisition.

Conflicts of interest

There are no conflicts of interest to declare.

Acknowledgements

References

1 F. Kawakubo, R. Morato, M. Martins, G. Mataveli, P. Nepomuceno and M. Martines, Quantification and Analysis of Impervious Surface Area in the Metropolitan Region of São Paulo, Brazil, *Remote Sens.*, 2019, **11**(8), 944, DOI: **10.3390/rs11080944**.

2 W. Jiang, D. Haver, M. Rust and J. Gan, Runoff of Pyrethroid Insecticides from Concrete Surfaces Following Simulated and Natural Rainfalls, *Water Res.*, 2012, **46**(3), 645–652, DOI: **10.1016/j.watres.2011.11.023**.

3 L. H. Nowell, P. W. Moran, R. J. Gilliom, D. L. Calhoun, C. G. Ingersoll, N. E. Kemble, K. M. Kuivila and P. J. Phillips, Contaminants in Stream Sediments From Seven United States Metropolitan Areas: Part I: Distribution in Relation to Urbanization, *Arch. Environ. Contam. Toxicol.*, 2013, **64**(1), 32–51, DOI: **10.1007/s00244-012-9813-0**.

4 L. Mutzner, K. Zhang, R. G. Luthy, H. P. H. Arp and S. Spahr, Urban Stormwater Capture for Water Supply: Look out for Persistent, Mobile and Toxic Substances, *Environ. Sci.: Water Res. Technol.*, 2023, **9**(12), 3094–3102, DOI: **10.1039/D3EW00160A**.

5 M. Lapointe, C. M. Rochman and N. Tufenkji, Sustainable Strategies to Treat Urban Runoff Needed, *Nat. Sustain.*, 2022, **5**, 366–369, DOI: **10.1038/s41893-022-00853-4**.

6 C. M. Rodak, T. L. Moore, R. David, A. D. Jayakaran and J. R. Vogel, Urban Stormwater Characterization, Control, and Treatment, *Water Environ. Res.*, 2019, **91**(10), 1034–1060, DOI: **10.1002/wer.1173**.

7 J. M. A. Gunawardena, A. Liu, P. Egodawatta, G. A. Ayoko, A. Goonetilleke, J. M. A. Gunawardena, A. Liu, P. Egodawatta, G. A. Ayoko and A. Goonetilleke, Predicting Stormwater Quality Resulting from Traffic Generated Pollutants, in *Influence of Traffic and Land Use on Urban Stormwater Quality: Implications for Urban Stormwater Treatment Design*, 2018, pp. 55–69, DOI: **10.1007/978-981-10-5302-3_4**.

8 J. R. Masoner, D. W. Kolpin, I. M. Cozzarelli, L. B. Barber, D. S. Burden, W. T. Foreman, K. J. Forshay, E. T. Furlong, J. F. Groves, M. L. Hladik, M. E. Hopton, J. B. Jaeschke, S. H. Keefe, D. P. Krabbenhoft, R. Lowrance, K. M. Romanok, D. L. Rus, W. R. Selbig, B. H. Williams and P. M. Bradley, Urban Stormwater: An Overlooked Pathway of Extensive Mixed Contaminants to Surface and Groundwaters in the United States, *Environ. Sci. Technol.*, 2019, **53**(17), 10070–10081, DOI: **10.1021/acs.est.9b02867**.

9 A. Goonetilleke and J. L. Lampard, *Stormwater Quality, Pollutant Sources, Processes, and Treatment Options, Approaches to Water Sensitive Urban Design*, Woodhead Publishing, 2019, pp. 49–74, DOI: **10.1016/B978-0-12-812843-5.00003-4**.

10 J. A. Charbonnet, Y. Duan, C. M. van Genuchten and D. L. Sedlak, Chemical Regeneration of Manganese Oxide-Coated Sand for Oxidation of Organic Stormwater Contaminants, *Environ. Sci. Technol.*, 2018, **52**(18), 10728–10736, DOI: **10.1021/acs.est.8b03304**.

11 S. J. Gaffield, R. L. Goo, L. A. Richards and R. J. Jackson, Public Health Effects of Inadequately Managed Stormwater Runoff, *Am. J. Public Health*, 2003, **93**(9), 1527–1533, DOI: **10.2105/AJPH.93.9.1527**.

12 J. R. Masoner, D. W. Kolpin, I. M. Cozzarelli, L. B. Barber, D. S. Burden, W. T. Foreman, K. J. Forshay, E. T. Furlong, J. F. Groves, M. L. Hladik, M. E. Hopton, J. B. Jaeschke, S. H. Keefe, D. P. Krabbenhoft, R. Lowrance, K. M. Romanok, D. L. Rus, W. R. Selbig, B. H. Williams and P. M. Bradley, Urban Stormwater: An Overlooked Pathway of Extensive Mixed Contaminants to Surface and Groundwaters in the United States, *Environ. Sci. Technol.*, 2019, **53**(17), 10070–10081, DOI: **10.1021/acs.est.9b02867**.

13 E. A. Wiener and G. H. LeFevre, White Rot Fungi Produce Novel Tire Wear Compound Metabolites and Reveal Underappreciated Amino Acid Conjugation Pathways,

Environ. Sci. Technol. Lett., 2022, **9**(5), 391–399, DOI: **10.1021/acs.estlett.2c00114**.

14 Z. Tian, H. Zhao, K. T. Peter, M. Gonzalez, J. Wetzel, C. Wu, X. Hu, J. Prat, E. Mudrock, R. Hettinger, A. E. Cortina, R. G. Biswas, F. V. C. Kock, R. Soong, A. Jenne, B. Du, F. Hou, H. He, R. Lundeen, A. Gilbreath, R. Sutton, N. L. Scholz, J. W. Davis, M. C. Dodd, A. Simpson, J. K. McIntyre and E. P. Kolodziej, A Ubiquitous Tire Rubber–Derived Chemical Induces Acute Mortality in Coho Salmon, *Science*, 2021, **371**(6525), 185–189, DOI: **10.1126/science.abd6951**.

15 C. Chen, W. Guo and H. H. Ngo, Pesticides in Stormwater Runoff—A Mini Review, *Front. Environ. Sci. Eng.*, 2019, **13**(5), 1–12.

16 K. D. Carpenter, K. M. Kuivila, M. L. Hladik, T. Haluska and M. B. Cole, Storm-Event-Transport of Urban-Use Pesticides to Streams Likely Impairs Invertebrate Assemblages, *Environ. Monit. Assess.*, 2016, **188**(6), 345, DOI: **10.1007/s10661-016-5215-5**.

17 J. M. Wolfand, C. Seller, C. D. Bell, Y.-M. Cho, K. Oetjen, T. S. Hogue and R. G. Luthy, Occurrence of Urban-Use Pesticides and Management with Enhanced Stormwater Control Measures at the Watershed Scale, *Environ. Sci. Technol.*, 2019, **53**(7), 3634–3644.

18 D. W. Schindler, S. R. Carpenter, S. C. Chapra, R. E. Hecky and D. M. Orihel, Reducing Phosphorus to Curb Lake Eutrophication Is a Success, *Environ. Sci. Technol.*, 2016, **50**(17), 8923–8929, DOI: **10.1021/acs.est.6b02204**.

19 I. Md Meftaul, K. Venkateswarlu, R. Dharmarajan, P. Annamalai and M. Megharaj, Pesticides in the Urban Environment: A Potential Threat That Knocks at the Door, *Sci. Total Environ.*, 2020, **711**, 134612, DOI: **10.1016/j.scitotenv.2019.134612**.

20 US EPA, DEET, US EPA, **https://www.epa.gov/insect-repellents/deet#:~:text=DEET%20chemical%20name%2C%20N%2C,ingredient%20in%20many%20repellent%20products**, (accessed 2024-05-05).

21 S. Y. Wee and A. Z. Aris, Revisiting the "Forever Chemicals", PFOA and PFOS Exposure in Drinking Water, *npj Clean Water*, 2023, **6**(1), 57, DOI: **10.1038/s41545-023-00274-6**.

22 K. M. Hawkins, J. C. Pritchard, S. Struck, Y.-M. Cho, R. G. Luthy and C. P. Higgins, Controlling Saturation to Improve Per- and Polyfluoroalkyl Substance (PFAS) Removal in Biochar-Amended Stormwater Bioretention Systems, *Environ. Sci.*, 2024, **10**(5), 1233–1244, DOI: **10.1039/D3EW00767G**.

23 J. Liu, D. J. Sample, C. Bell and Y. Guan, Review and Research Needs of Bioretention Used for the Treatment of Urban Stormwater, *Water*, 2014, **6**(4), 1069–1099, DOI: **10.3390/w6041069**.

24 C. Jiang, J. Li, H. Li, Y. Li and L. Chen, Field Performance of Bioretention Systems for Runoff Quantity Regulation and Pollutant Removal, *Water, Air, Soil Pollut.*, 2017, **228**(12), 468, DOI: **10.1007/s11270-017-3636-6**.

25 G. H. LeFevre, M. D. Hendricks, M. E. Carrasquillo, L. E. McPhillips, B. K. Winfrey and J. R. Mihelcic, The Greatest Opportunity for Green Stormwater Infrastructure Is to Advance Environmental Justice, *Environ. Sci. Technol.*, 2023, **57**(48), 19088–19093, DOI: **10.1021/acs.est.3c07062**.

26 US EPA, Going Wild: the Conservation Co-benefits of Green Infrastructure, US EPA, **https://www.epa.gov/green-infrastructure/going-wild-conservation-co-benefits-green-infrastructure#:~:text=Green%20infrastructure%20offers%20tools%20that,to%20the%20places%20we%20live**, (accessed 2024-04-30).

27 T. F. M. Rodgers, L. Wu, X. Gu, S. Spraakman, E. Passeport and M. L. Diamond, Stormwater Bioretention Cells Are Not an Effective Treatment for Persistent and Mobile Organic Compounds (PMOCs), *Environ. Sci. Technol.*, 2022, **56**(10), 6349–6359, DOI: **10.1021/acs.est.1c07555**.

28 C. M. Rodak, T. L. Moore, R. David, A. D. Jayakaran and J. R. Vogel, Urban Stormwater Characterization, Control, and Treatment, *Water Environ. Res.*, 2019, **91**(10), 1034–1060, DOI: **10.1002/wer.1173**.

29 Y. Zhang, A. Skorobogatov, J. He, C. Valeo, A. Chu, B. van Duin and L. van Duin, Mitigation of Nutrient Leaching from Bioretention Systems Using Amendments, *J. Hydrol.*, 2023, **618**, 129182, DOI: **10.1016/j.jhydrol.2023.129182**.

30 H. Smaili and C. Ng, Adsorption as a Remediation Technology for Short-Chain per- and Polyfluoroalkyl Substances (PFAS) from Water – a Critical Review, *Environ. Sci.*, 2023, **9**(2), 344–362, DOI: **10.1039/D2EW00721E**.

31 B. A. Ulrich, M. Loehnert and C. P. Higgins, Improved Contaminant Removal in Vegetated Stormwater Biofilters Amended with Biochar, *Environ. Sci.: Water Res. Technol.*, 2017, **3**(4), 726–734, DOI: **10.1039/c7ew00070g**.

32 B. A. Ulrich, E. A. Im, D. Werner and C. P. Higgins, Biochar and Activated Carbon for Enhanced Trace Organic Contaminant Retention in Stormwater Infiltration Systems, *Environ. Sci. Technol.*, 2015, **49**(10), 6222–6230, DOI: **10.1021/acs.est.5b00376**.

33 A. B. Boehm, C. D. Bell, N. J. M. Fitzgerald, E. Gallo, C. P. Higgins, T. S. Hogue, R. G. Luthy, A. C. Portmann, B. A. Ulrich and J. M. Wolfand, Biochar-Augmented Biofilters to Improve Pollutant Removal from Stormwater – Can They Improve Receiving Water Quality?, *Environ. Sci.: Water Res. Technol.*, 2020, **6**(6), 1520–1537, DOI: **10.1039/D0EW00027B**.

34 A. J. Erickson, J. S. Gulliver and P. T. Weiss, Capturing Phosphates with Iron Enhanced Sand Filtration, *Water Res.*, 2012, **46**(9), 3032–3042, DOI: **10.1016/j.watres.2012.03.009**.

35 J. A. Ippolito, K. A. Barbarick and H. A. Elliott, Drinking Water Treatment Residuals: A Review of Recent Uses, *J. Environ. Qual.*, 2011, **40**(1), 1–12, DOI: **10.2134/jeq2010.0242**.

36 M. Likus, M. Komorowska-Kaufman, A. Pruss, Ł. Zych and T. Bajda, Iron-Based Water Treatment Residuals: Phase, Physicochemical Characterization, and Textural Properties, *Materials*, 2021, **14**(14), 3938, DOI: **10.3390/ma14143938**.

37 C. Wang, W. Guo, B. Tian, Y. Pei and K. Zhang, Characteristics and Kinetics of Phosphate Adsorption on Dewatered Ferric-Alum Residuals, *J. Environ. Sci. Health, Part A: Toxic/Hazard. Subst. Environ. Eng.*, 2011, **46**(14), 1632–1639, DOI: **10.1080/10934529.2011.623643**.

This journal is © The Royal Society of Chemistry 2024

Environ. Sci.: Water Res. Technol., 2024, **10**, 3339–3357 | **3353**

38 T. F. M. Rodgers, S. Spraakman, Y. Wang, C. Johannessen, R. C. Scholes and A. Giang, Bioretention Design Modifications Increase the Simulated Capture of Hydrophobic and Hydrophilic Trace Organic Compounds, *Environ. Sci. Technol.*, 2024, **58**(12), 5500–5511, DOI: **10.1021/acs.est.3c10375**.

39 D. Laird, P. Fleming, B. Wang, R. Horton and D. Karlen, Biochar Impact on Nutrient Leaching from a Midwestern Agricultural Soil, *Geoderma*, 2010, **158**(3), 436–442, DOI: **10.1016/j.geoderma.2010.05.012**.

40 S. M. Elliott, R. L. Kiesling, A. M. Berg and H. L. Schoenfuss, A Pilot Study to Assess the Influence of Infiltrated Stormwater on Groundwater: Hydrology and Trace Organic Contaminants, *Water Environ. Res.*, 2022, **94**(2), e10690, DOI: **10.1002/wer.10690**.

41 A. Zubair, A. Hussain, M. A. Farooq and H. N. Abbasi, Impact of Storm Water on Groundwater Quality below Retention/Detention Basins, *Environ. Monit. Assess.*, 2010, **162**(1–4), 427–437, DOI: **10.1007/s10661-009-0807-y**.

42 A. C. Portmann, G. H. LeFevre, R. Hankawa, D. Werner and C. P. Higgins, The Regenerative Role of Biofilm in the Removal of Pesticides from Stormwater in Biochar-Amended Biofilters, *Environ. Sci.: Water Res. Technol.*, 2022, **8**(5), 1092–1110, DOI: **10.1039/D1EW00870F**.

43 J. M. Wolfand, G. H. LeFevre and R. G. Luthy, Metabolization and Degradation Kinetics of the Urban-Use Pesticide Fipronil by White Rot Fungus Trametes Versicolor, *Environ. Sci.: Processes Impacts*, 2016, **18**(10), 1256–1265, DOI: **10.1039/C6EM00344C**.

44 E. A. Wiener, J. M. Ewald and G. H. LeFevre, Fungal Diversity and Key Functional Gene Abundance in Iowa Bioretention Cells: Implications for Stormwater Remediation Potential, *Environ. Sci.: Processes Impacts*, 2024, **26**(10), 1796–1810, DOI: **10.1039/D4EM00275J**.

45 D. S. Tanmoy and G. H. LeFevre, Development of Composite Alginate Bead Media with Encapsulated Sorptive Materials and Microorganisms to Bioaugment Green Stormwater Infrastructure, *Environ. Sci.*, 2024, **10**, 1890–1907, DOI: **10.1039/D4EW00289J**.

46 Z. Kong, Y. Song, M. Xu, Y. Yang, X. Wang, H. Ma, Y. Zhi, Z. Shao, L. Chen, Y. Yuan, F. Liu, Y. Xu, Q. Ni, S. Hu and H. Chai, Multi-Media Interaction Improves the Efficiency and Stability of the Bioretention System for Stormwater Runoff Treatment, *Water Res.*, 2024, **250**, 121017, DOI: **10.1016/j.watres.2023.121017**.

47 Minnesota Pollution Control Agency (MPCA), Minnesota Stormwater Manual, **https://stormwater.pca.state.mn.us/index.php?title=Main_Page**, (accessed 2024-06-03).

48 A. R. Prestigiacomo, S. W. Effler, R. K. Gelda, D. A. Matthews, M. T. Auer, B. E. Downer, A. Kuczynski and M. T. Walter, Apportionment of Bioavailable Phosphorus Loads Entering Cayuga Lake, New York, *J. Am. Water Resour. Assoc.*, 2016, **52**(1), 31–47, DOI: **10.1111/1752-1688.12366**.

49 B. Zhou, C. Parsons and P. Van Cappellen, Urban Stormwater Phosphorus Export Control: Comparing Traditional and Low-Impact Development Best Management Practices, *Environ. Sci. Technol.*, 2024, **58**(26), 11376–11385, DOI: **10.1021/acs.est.4c01705**.

50 Q. Jia, B. Li, B. Li, Y. Cai and X. Yuan, Experiments and Simulation of Adsorption Characteristics of Typical Neonicotinoids in Urban Stream Sediments, *Environ. Sci. Pollut. Res.*, 2023, **30**(31), 76992–77005, DOI: **10.1007/s11356-023-27025-x**.

51 J. Xiong, Z. Wang, X. Ma, H. Li and J. You, Occurrence and Risk of Neonicotinoid Insecticides in Surface Water in a Rapidly Developing Region: Application of Polar Organic Chemical Integrative Samplers, *Sci. Total Environ.*, 2019, **648**, 1305–1312, DOI: **10.1016/j.scitotenv.2018.08.256**.

52 D. T. Webb, M. R. Nagorzanski, M. M. Powers, D. M. Cwiertny, M. L. Hladik and G. H. LeFevre, Differences in Neonicotinoid and Metabolite Sorption to Activated Carbon Are Driven by Alterations to the Insecticidal Pharmacophore, *Environ. Sci. Technol.*, 2020, **54**(22), 14694–14705, DOI: **10.1021/acs.est.0c04187**.

53 P. Zhang, C. Ren, H. Sun and L. Min, Sorption, Desorption and Degradation of Neonicotinoids in Four Agricultural Soils and Their Effects on Soil Microorganisms, *Sci. Total Environ.*, 2018, **615**, 59–69, DOI: **10.1016/j.scitotenv.2017.09.097**.

54 M. L. Hladik, D. W. Kolpin and K. M. Kuivila, Widespread Occurrence of Neonicotinoid Insecticides in Streams in a High Corn and Soybean Producing Region, USA, *Environ. Pollut.*, 2014, **193**, 189–196, DOI: **10.1016/j.envpol.2014.06.033**.

55 M. K. Gibbons and G. A. Gagnon, Understanding Removal of Phosphate or Arsenate onto Water Treatment Residual Solids, *J. Hazard. Mater.*, 2011, **186**(2), 1916–1923, DOI: **10.1016/j.jhazmat.2010.12.085**.

56 M. B. Asif, F. I. Hai, L. Singh, W. E. Price and L. D. Nghiem, Degradation of Pharmaceuticals and Personal Care Products by White-Rot Fungi—a Critical Review, *Curr. Pollut. Rep.*, 2017, **3**(2), 88–103, DOI: **10.1007/s40726-017-0049-5**.

57 S. Wang, W. Li, L. Liu, H. Qi and H. You, Biodegradation of Decabromodiphenyl Ethane (DBDPE) by White-Rot Fungus Pleurotus Ostreatus: Characteristics, Mechanisms, and Toxicological Response, *J. Hazard. Mater.*, 2022, **424**, 127716, DOI: **10.1016/j.jhazmat.2021.127716**.

58 W. Zhou, X. Chen, M. Ismail, L. Wei and B. Hu, Simulating the Synergy of Electron Donors and Different Redox Mediators on the Anaerobic Decolorization of Azo Dyes: Can AQDS-Chitosan Globules Replace the Traditional Redox Mediators?, *Chemosphere*, 2021, **275**, 130025, DOI: **10.1016/j.chemosphere.2021.130025**.

59 A. K. Loomis, A. M. Childress, D. Daigle and J. W. Bennett, Alginate Encapsulation of the White Rot Fungus Phanerochaete Chrysosporium, *Curr. Microbiol.*, 1997, **34**(2), 127–130, DOI: **10.1007/s002849900156**.

60 K. L. Klarich Wong, D. T. Webb, M. R. Nagorzanski, D. W. Kolpin, M. L. Hladik, D. M. Cwiertny and G. H. LeFevre, Chlorinated Byproducts of Neonicotinoids and Their Metabolites: An Unrecognized Human Exposure Potential?,

3354 | *Environ. Sci.: Water Res. Technol.*, 2024, **10**, 3339–3357

This journal is © The Royal Society of Chemistry 2024

Environ. Sci. Technol. Lett., 2019, **6**(2), 98–105, DOI: **10.1021/acs.estlett.8b00706**.

61 L. M. M. Weaver, N. L. Alexander, M. A. Cubeta, D. R. U. Knappe and T. N. Aziz, Degradation of Imidacloprid by Phanerodontia Chrysosporium on Wood Chips for Stormwater Treatment, *Environ. Sci.*, 2023, **9**(12), 3333–3343, DOI: **10.1039/D3EW00545C**.

62 N. Lambert, P. Van Aken, R. Van den Broeck and R. Dewil, Adsorption of Phosphate on Iron-Coated Sand Granules as a Robust End-of-Pipe Purification Strategy in the Horticulture Sector, *Chemosphere*, 2021, **267**, 129276, DOI: **10.1016/j.chemosphere.2020.129276**.

63 A. J. Erickson, J. S. Gulliver and P. T. Weiss, Capturing Phosphates with Iron Enhanced Sand Filtration, *Water Res.*, 2012, **46**(9), 3032–3042, DOI: **10.1016/j.watres.2012.03.009**.

64 H. Ai, K. Zhang, C. J. Penn and H. Zhang, Phosphate Removal by Low-Cost Industrial Byproduct Iron Shavings: Efficacy and Longevity, *Water Res.*, 2023, **246**, 120745, DOI: **10.1016/j.watres.2023.120745**.

65 M. K. Gibbons and G. A. Gagnon, Understanding Removal of Phosphate or Arsenate onto Water Treatment Residual Solids, *J. Hazard. Mater.*, 2011, **186**(2), 1916–1923, DOI: **10.1016/j.jhazmat.2010.12.085**.

66 Z. Isik, M. Saleh and N. Dizge, Adsorption Studies of Ammonia and Phosphate Ions onto Calcium Alginate Beads, *Surf. Interfaces*, 2021, **26**, 101330, DOI: **10.1016/j.surfin.2021.101330**.

67 H. Siwek, A. Bartkowiak, M. Włodarczyk and K. Sobecka, Removal of Phosphate from Aqueous Solution Using Alginate/Iron (III) Chloride Capsules: A Laboratory Study, *Water, Air, Soil Pollut.*, 2016, **227**(11), 427, DOI: **10.1007/s11270-016-3128-0**.

68 M. d. C. Gutiérrez, F. J. García-Mateos, R. Ruiz-Rosas, J. M. Rosas, J. Rodríguez-Mirasol and T. Cordero, Evaluation of Acetanilide and Antipyrine Adsorption on Lignin-Derived Activated Carbons, *Environ. Res.*, 2024, **252**, 118918, DOI: **10.1016/j.envres.2024.118918**.

69 D. T. Webb, M. R. Nagorzanski, D. M. Cwiertny and G. H. LeFevre, Combining Experimental Sorption Parameters with QSAR to Predict Neonicotinoid and Transformation Product Sorption to Carbon Nanotubes and Granular Activated Carbon, *ACS ES&T Water*, 2022, **2**(1), 247–258, DOI: **10.1021/acsestwater.1c00492**.

70 S. Mopoung, P. Moonsri, W. Palas and S. Khumpai, Characterization and Properties of Activated Carbon Prepared from Tamarind Seeds by KOH Activation for Fe(III) Adsorption from Aqueous Solution, *Sci. World J.*, 2015, **2015**, 415961, DOI: **10.1155/2015/415961**.

71 M. Hassan, Y. Liu, R. Naidu, S. J. Parikh, J. Du, F. Qi and I. R. Willett, Influences of Feedstock Sources and Pyrolysis Temperature on the Properties of Biochar and Functionality as Adsorbents: A Meta-Analysis, *Sci. Total Environ.*, 2020, **744**, 140714, DOI: **10.1016/j.scitotenv.2020.140714**.

72 B. Wang, Y. Wan, Y. Zheng, X. Lee, T. Liu, Z. Yu, J. Huang, Y. S. Ok, J. Chen and B. Gao, Alginate-Based Composites for Environmental Applications: A Critical Review, *Crit. Rev. Environ. Sci. Technol.*, 2019, **49**(4), 318–356, DOI: **10.1080/10643389.2018.1547621**.

73 A. Shalapy, S. Zhao, C. Zhang, Y. Li, H. Geng, S. Ullah, G. Wang, S. Huang and Y. Liu, Adsorption of Deoxynivalenol (DON) from Corn Steep Liquor (CSL) by the Microsphere Adsorbent SA/CMC Loaded with Calcium, *Toxins*, 2020, **12**(4), 208, DOI: **10.3390/toxins12040208**.

74 I. Garbayo, R. León and C. Vílchez, Diffusion Characteristics of Nitrate and Glycerol in Alginate, *Colloids Surf., B*, 2002, **25**(1), 1–9, DOI: **10.1016/S0927-7765(01)00287-9**.

75 M. Tomizawa and J. E. Casida, Selective Toxicity of Neonicotinoids Attributable to Specificity of Insect and Mammalian Nicotinic Receptors, *Annu. Rev. Entomol.*, 2003, **48**(1), 339–364, DOI: **10.1146/annurev.ento.48.091801.112731**.

76 H. Malektaj, A. D. Drozdov and J. deClaville Christiansen, Mechanical Properties of Alginate Hydrogels Cross-Linked with Multivalent Cations, *Polymers*, 2023, **15**(14), 3012, DOI: **10.3390/polym15143012**.

77 D. Massana Roquero, A. Othman, A. Melman and E. Katz, Iron(Iii)-Cross-Linked Alginate Hydrogels: A Critical Review, *Mater. Adv.*, 2022, **3**(4), 1849–1873, DOI: **10.1039/D1MA00959A**.

78 H. H. Tønnesen and J. Karlsen, Alginate in Drug Delivery Systems, *Drug Dev. Ind. Pharm.*, 2002, **28**(6), 621–630, DOI: **10.1081/DDC-120003853**.

79 S.-K. Ahn, K.-Y. Park, W. Song, Y. Park and J.-H. Kweon, Adsorption Mechanisms on Perfluorooctanoic Acid by FeCl3 Modified Granular Activated Carbon in Aqueous Solutions, *Chemosphere*, 2022, **303**, 134965, DOI: **10.1016/j.chemosphere.2022.134965**.

80 H. Lin, Y. Wang, J. Niu, Z. Yue and Q. Huang, Efficient Sorption and Removal of Perfluoroalkyl Acids (PFAAs) from Aqueous Solution by Metal Hydroxides Generated in Situ by Electrocoagulation, *Environ. Sci. Technol.*, 2015, **49**(17), 10562–10569, DOI: **10.1021/acs.est.5b02092**.

81 Z. Zhang, D. Sarkar, R. Datta and Y. Deng, Adsorption of Perfluorooctanoic Acid (PFOA) and Perfluorooctanesulfonic Acid (PFOS) by Aluminum-Based Drinking Water Treatment Residuals, *J. Hazard. Mater. Lett.*, 2021, **2**, 100034, DOI: **10.1016/j.hazl.2021.100034**.

82 D. Ordonez, A. Valencia, A. H. M. A. Sadmani and N.-B. Chang, Green Sorption Media for the Removal of Perfluorooctanesulfonic Acid (PFOS) and Perfluorooctanoic Acid (PFOA) from Water, *Sci. Total Environ.*, 2022, **819**, 152886, DOI: **10.1016/j.scitotenv.2021.152886**.

83 Z. Du, S. Deng, Y. Bei, Q. Huang, B. Wang, J. Huang and G. Yu, Adsorption Behavior and Mechanism of Perfluorinated Compounds on Various Adsorbents—A Review, *J. Hazard. Mater.*, 2014, **274**, 443–454, DOI: **10.1016/j.jhazmat.2014.04.038**.

84 Agency for Toxic Substances and Disease Registry (US), Physical and Chemical Properties of Perfluoroalkyls, Atlanta (GA), **https://doi.org/10.15620/cdc:59198**.

This journal is © The Royal Society of Chemistry 2024

Environ. Sci.: Water Res. Technol., 2024, **10**, 3339–3357 | **3355**

85 B. Niu, S. Yang, Y. Li, K. Zang, C. Sun, M. Yu, L. Zhou and Y. Zheng, Regenerable Magnetic Carbonized Calotropis Gigantea Fiber for Hydrophobic-Driven Fast Removal of Perfluoroalkyl Pollutants, *Cellulose*, 2020, **27**(10), 5893–5905, DOI: **10.1007/s10570-020-03192-9**.

86 Z. Du, S. Deng, Y. Bei, Q. Huang, B. Wang, J. Huang and G. Yu, Adsorption Behavior and Mechanism of Perfluorinated Compounds on Various Adsorbents—A Review, *J. Hazard. Mater.*, 2014, **274**, 443–454, DOI: **10.1016/j.jhazmat.2014.04.038**.

87 F. Wang, C. Liu and K. Shih, Adsorption Behavior of Perfluorooctanesulfonate (PFOS) and Perfluorooctanoate (PFOA) on Boehmite, *Chemosphere*, 2012, **89**(8), 1009–1014, DOI: **10.1016/j.chemosphere.2012.06.071**.

88 S. P. Lenka, M. Kah, J. L.-Y. Chen, B. A. Tiban-Anrango and L. P. Padhye, Adsorption Mechanisms of Short-Chain and Ultrashort-Chain PFAS on Anion Exchange Resins and Activated Carbon, *Environ. Sci.*, 2024, **10**(5), 1280–1293, DOI: **10.1039/D3EW00959A**.

89 S. Sánchez López, J. MacAdam, M. Biddle and P. Jarvis, The Impact of Dosing Sequence on the Removal of the Persistent Pesticide Metaldehyde Using Powdered Activated Carbon with Coagulation and Clarification, *J. Water Process Eng.*, 2021, **39**, 101756, DOI: **10.1016/j.jwpe.2020.101756**.

90 M. V. Tuttolomondo, G. S. Alvarez, M. F. Desimone and L. E. Diaz, Removal of Azo Dyes from Water by Sol–Gel Immobilized Pseudomonas Sp., *J. Environ. Chem. Eng.*, 2014, **2**(1), 131–136, DOI: **10.1016/j.jece.2013.12.003**.

91 K. Doukani, D. Boukirat, A. Boumezrag, H. Bouhenni and Y. Bounouira, Biodegradation of Pollutants, in *Handbook of Biodegradable Materials*, ed. G. A. M. Ali and A. S. H. Makhlouf, Springer International Publishing, Cham, 2022, pp. 1–27, DOI: **10.1007/978-3-030-83783-9_10-1**.

92 H. D. Rizqi, A. S. Purnomo and A. Ulfi, The Effect of Bacteria Addition on DDT Biodegradation by BROWN-ROT Fungus Gloeophyllum Trabeum, *Heliyon*, 2023, **9**(7), e18216, DOI: **10.1016/j.heliyon.2023.e18216**.

93 N. Khan, E. Muge, F. J. Mulaa, B. Wamalwa, M. von Bergen, N. Jehmlich and L. Y. Wick, Mycelial Nutrient Transfer Promotes Bacterial Co-Metabolic Organochlorine Pesticide Degradation in Nutrient-Deprived Environments, *ISME J.*, 2023, **17**(4), 570–578, DOI: **10.1038/s41396-023-01371-7**.

94 Y. Dinakarkumar, G. Ramakrishnan, K. R. Gujjula, V. Vasu, P. Balamurugan and G. Murali, Fungal Bioremediation: An Overview of the Mechanisms, Applications and Future Perspectives, *Environ. Chem. Ecotoxicol.*, 2024, **6**, 293–302, DOI: **10.1016/j.enceco.2024.07.002**.

95 Y. M. Palacios, R. Gleadow, C. Davidson, W. Gan and B. Winfrey, Do Mycorrhizae Increase Plant Growth and Pollutant Removal in Stormwater Biofilters?, *Water Res.*, 2021, **202**, 117381, DOI: **10.1016/j.watres.2021.117381**.

96 D. S. Tanmoy, J. C. Bezares-Cruz and G. H. LeFevre, The Use of Recycled Materials in a Biofilter to Polish Anammox Wastewater Treatment Plant Effluent, *Chemosphere*, 2022, **296**, 134058, DOI: **10.1016/j.chemosphere.2022.134058**.

97 X. Chen, E. Peltier, B. S. M. Sturm and C. B. Young, Nitrogen Removal and Nitrifying and Denitrifying Bacteria Quantification in a Stormwater Bioretention System, *Water Res.*, 2013, **47**(4), 1691–1700, DOI: **10.1016/j.watres.2012.12.033**.

98 S. L. Woods, D. J. Trobaugh and K. J. Carter, Polychlorinated Biphenyl Reductive Dechlorination by Vitamin B12s: Thermodynamics and Regiospecificity, *Environ. Sci. Technol.*, 1999, **33**(6), 857–863, DOI: **10.1021/es9804823**.

99 S. Huang and P. R. Jaffé, Defluorination of Perfluorooctanoic Acid (PFOA) and Perfluorooctane Sulfonate (PFOS) by Acidimicrobium Sp. Strain A6, *Environ. Sci. Technol.*, 2019, **53**(19), 11410–11419, DOI: **10.1021/acs.est.9b04047**.

100 B. Anegbe, I. H. Ifijen, M. Maliki, I. E. Uwidia and A. I. Aigbodion, Graphene Oxide Synthesis and Applications in Emerging Contaminant Removal: A Comprehensive Review, *Environ. Sci. Eur.*, 2024, **36**(1), 15, DOI: **10.1186/s12302-023-00814-4**.

101 K. Q. Jabbar, A. A. Barzinjy and S. M. Hamad, Iron Oxide Nanoparticles: Preparation Methods, Functions, Adsorption and Coagulation/Flocculation in Wastewater Treatment, *Environ. Nanotechnol., Monit. Manage.*, 2022, **17**, 100661, DOI: **10.1016/j.enmm.2022.100661**.

102 S. Vahidhabanu, D. Karuppasamy, A. I. Adeogun and B. R. Babu, Impregnation of Zinc Oxide Modified Clay over Alginate Beads: A Novel Material for the Effective Removal of Congo Red from Wastewater, *RSC Adv.*, 2017, **7**(10), 5669–5678, DOI: **10.1039/C6RA26273B**.

103 J. A. Leiva, P. C. Wilson, J. P. Albano, P. Nkedi-Kizza and G. A. O'Connor, Pesticide Sorption to Soilless Media Components Used for Ornamental Plant Production and Aluminum Water Treatment Residuals, *ACS Omega*, 2019, **4**(18), 17782–17790, DOI: **10.1021/acsomega.9b02296**.

104 Z. Si, X. Song, Y. Wang, X. Cao, Y. Zhao, B. Wang, Y. Chen and A. Arefe, Intensified Heterotrophic Denitrification in Constructed Wetlands Using Four Solid Carbon Sources: Denitrification Efficiency and Bacterial Community Structure, *Bioresour. Technol.*, 2018, **267**, 416–425, DOI: **10.1016/j.biortech.2018.07.029**.

105 B. Zhou, J. Duan, L. Xue, J. Zhang and L. Yang, Effect of Plant-Based Carbon Source Supplements on Denitrification of Synthetic Wastewater: Focus on the Microbiology, *Environ. Sci. Pollut. Res.*, 2019, **26**(24), 24683–24694, DOI: **10.1007/s11356-019-05454-x**.

106 A. Okamoto, S. Kalathil, X. Deng, K. Hashimoto, R. Nakamura and K. H. Nealson, Cell-Secreted Flavins Bound to Membrane Cytochromes Dictate Electron Transfer Reactions to Surfaces with Diverse Charge and PH, *Sci. Rep.*, 2014, **4**(1), 5628, DOI: **10.1038/srep05628**.

107 L. Klüpfel, M. Keiluweit, M. Kleber and M. Sander, Redox Properties of Plant Biomass-Derived Black Carbon (Biochar), *Environ. Sci. Technol.*, 2014, **48**(10), 5601–5611, DOI: **10.1021/es500906d**.

108 Y. Gao, L. Ren, W. Ling, S. Gong, B. Sun and Y. Zhang, Desorption of Phenanthrene and Pyrene in Soils by Root Exudates, *Bioresour. Technol.*, 2010, **101**(4), 1159–1165, DOI: **10.1016/j.biortech.2009.09.062**.

3356 | *Environ. Sci.: Water Res. Technol.*, 2024, **10**, 3339–3357

This journal is © The Royal Society of Chemistry 2024

109 E. J. Joner, S. C. Corgié, N. Amellal and C. Leyval, Nutritional Constraints to Degradation of Polycyclic Aromatic Hydrocarbons in a Simulated Rhizosphere, *Soil Biol. Biochem.*, 2002, **34**(6), 859–864, DOI: **10.1016/S0038-0717(02)00018-4**.

This journal is © The Royal Society of Chemistry 2024

Environ. Sci.: Water Res. Technol., 2024, **10**, 3339–3357 | **3357**